DFT Mechanistic Insights into the Alkyne Insertion Reaction Affording Diiron μ-Vinyliminium Complexes and New Functionalization Pathways

Gianluca Ciancaleoni,[a,b,*] Stefano Zacchini,[b,c] Valerio Zanotti [b,c] and Fabio Marchetti [a,b,*]

[a] *University of Pisa, Dipartimento di Chimica e Chimica Industriale, Via G. Moruzzi 13, I-56124 Pisa, Italy*

[b] *CIRCC, Via Celso Ulpiani 27, I-70126 Bari, Italy.*

[c] *University of Bologna, Dipartimento di Chimica Industriale "Toso Montanari", Viale Risorgimento 4, I-40136 Bologna, Italy.*

Abstract

Insertion of propyne or 2-butyne into the Fe-carbyne bond belonging to the fragment $[Fe_2Cp_2(CO)(\mu\text{-}CO)\{\mu\text{-}CNMe(R)\}]^+$ (R = Me or Xyl = 2,6-$C_6H_3Me_2$) was DFT investigated, and plausible intermediates were identified along the formation of the vinyliminium complexes $[Fe_2Cp_2(CO)(\mu\text{-}CO)\{\mu\text{-}\eta^1\text{:}\eta^3\text{-}C(Me)C(R'')CN(Me)(R)\}]SO_3CF_3$, [**2a-d**]$^+$, thus allowing to explain regio- and stereochemical features. The X-ray structure of [**2a**]SO_3CF_3 (R = Me, R″ = H) was determined by single crystal X-ray diffraction.

Novel C-C and C-S bond forming pathways involving the vinyliminium ligand were then explored. Thus, [**2b**]SO_3CF_3 (R = Xyl, R″ = H) reacted with cyclopentadiene (or cyclopentene), triphenylphosphonium methylide and benzyl bromide, in tetrahydrofuran in the presence of sodium hydride, to give respectively $[Fe_2Cp_2(CO)(\mu\text{-}CO)\{\mu\text{-}\eta^1\text{:}\eta^2\text{-}C(Me)C\{C(CH)_4\}CN(Me)(Xyl)\}]$, **3**, $[Fe_2Cp_2(CO)(\mu\text{-}CO)\{\mu\text{-}\eta^1\text{:}\eta^2\text{-}C(Me)C(CH_2)CN(Me)(Xyl)\}]$, **4**, and $[Fe_2Cp_2(CO)(\mu\text{-}CO)\{\mu\text{-}\eta^1\text{:}\eta^3\text{-}C(Me)C(CH_2Ph)CN(Me)(Xyl)\}]Br$, [**5**]Br, in good yields. The unstable complex **4** (detected by IR spectroscopy) readily converted into [**2c**]SO_3CF_3 (R = Xyl, R″ = Me) upon HSO_3CF_3 protonation of the methylide function. [**5**]Br was obtained as E/Z isomeric mixture, which was then quantitatively converted into the most stable *Z* form, by heating in methanol solution at 50 °C. The reactions of [**2c-d**]SO_3CF_3 (R = Me, Xyl, R″ = Me) with PhSSPh/NaH selectively yielded the aminoalkylidyne species $[Fe_2Cp_2(SPh)(CO)(\mu\text{-}CO)\{\mu\text{-}CN(Me)(Xyl)\}]$, **6**, and the bis-alkylidene $[Fe_2Cp_2(CO)(\mu\text{-}CO)\{\mu\text{-}\eta^1\text{:}\eta^2\text{-}C(Me)C(Me)(SPh)CN(Me)_2\}]$, **7**, respectively, probably via the intermediacy of the radical compounds **2c-d**. The structures of **3-7** and **2c-d** were elucidated by DFT calculations, and the isolated products were characterized by analytical and spectroscopic methods.

Introduction

Alkynes are useful and versatile reagents in organometallic chemistry. They can behave as η^2 terminal ligands or occupy bridging sites in polynuclear complexes,[1] and this preliminary coordination may prelude to an impressive variety of reactions pathways.[2] In particular, the intramolecular alkyne insertion into a metal-carbon bond, in di- and tri-nuclear metal complexes, represents an intriguing strategy to grow various hydrocarbyl fragments stabilized by bridging multisite coordination.[3]

On the other hand, $[Fe_2Cp_2(CO)_4]$ is a long time known, easily available and robust compound,[4] previously used as a starting material for pioneering studies to explore new C–C bond coupling reactions and to model the Fischer Tropsch process.[5] The construction of organometallic motifs supported on the $[Fe_2Cp_2(CO)_x]$ skeleton has witnessed a renewed interest,[6] in view of the current huge effort to develop sustainable synthetic routes based on earth abundant metals,[7] and the awareness that Nature uses diiron organometallic units to perform amazingly-efficient enzymatic processes.[8]

Diiron compounds $[Fe_2Cp_2(CO)_3(L)]$ are known to undergo alkyne insertion between one Fe atom and the bridging L ligand, the latter being CO [9] or a fragment isolobal to CO (i.e., thiocarbonyl [10] or isocyanide [11]), see Scheme 1. This general reaction requires the preliminary photolytic displacement of one terminal carbonyl ligand, in order to generate a vacant site available to the entrance of the alkyne.

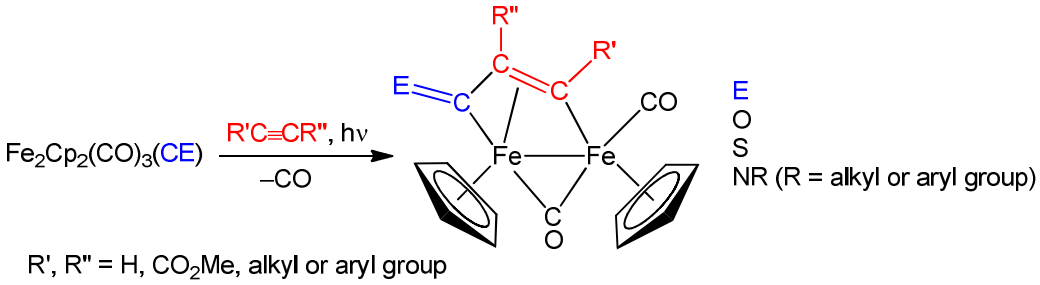

Scheme 1. Insertion reactions of alkynes into: iron-carbonyl (E = O);[9] iron-thiocarbonyl (E = S);[10] iron-isocyanide (E = NR).[11]

The analogous interaction of alkynes with aminoalkylidyne complexes, $[Fe_2Cp_2(CO)_2(\mu\text{-}CO)\{\mu\text{-}CNMe(R)\}]^+$ (R = Me, [**1a**]$^+$; R = Xyl = 2,6-$C_6H_3Me_2$, [**1b**]$^+$), benefits from the net cationic charge of the

complexes, weakening the terminal CO binding. Therefore, CO elimination is viable with a chemical approach, rather than with the much less selective photochemical method. More precisely, the required vacant site is conveniently generated removing one carbonyl with trimethylamine-N-oxide, and can be temporarily occupied by a labile acetonitrile ligand (or chloride, to be abstracted with a silver salt). The subsequent alkyne insertion into iron-carbyne bond, affording vinyliminium complexes, is usually regiospecific, i.e. placing the most hindered alkyne substituent (R') far from the newly generated iminium moiety.[12] The representative synthesis of [**2a-d**]$^+$ from [**1a-b**]$^+$ and propyne or 2-butyne, respectively, is shown in Scheme 2.

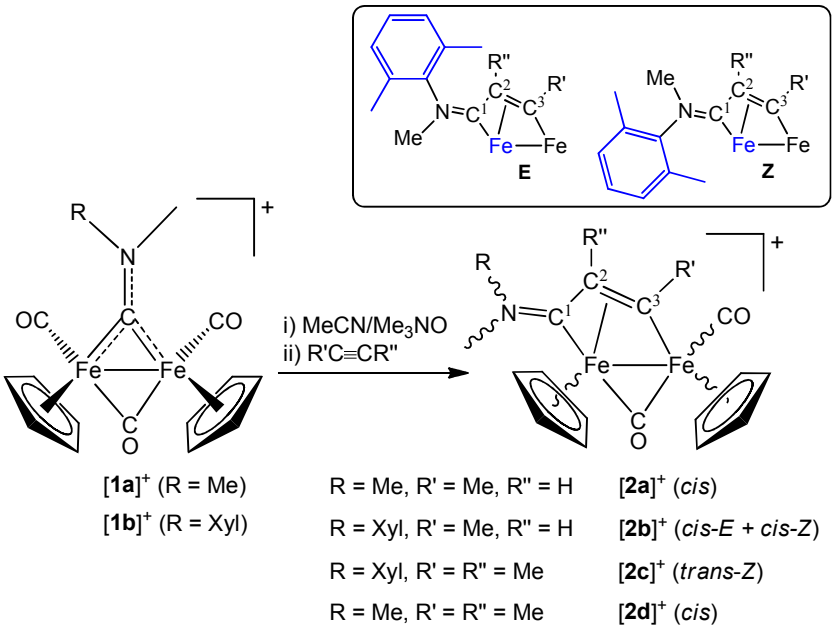

Scheme 2. Synthesis of vinyliminium complexes via i) generation of a coordination vacancy and ii) alkyne insertion into Fe-carbyne bond (Xyl = 2,6-$C_6H_3Me_2$). Inset: E/Z geometry around the iminium bond in [**2b-c**]$^+$.

The μ-vinyliminium ligand in [**2**]$^+$ displays a rather rare coordination fashion [13] and a rich reactivity, essentially related to the cationic charge of the complex and the cooperative effects provided by the two adjacent iron atoms.[14] Such reactivity ranges from nucleophilic additions,[15] incorporation of small molecular units,[16] and synthesis of unusually functionalized sandwich compounds [17] or other monoiron species.[18]

The mechanism of formation of diiron vinyliminium compounds [**2**]$^+$ is not obvious, for at least two reasons. First, iron-alkyne intermediates are likely but elusive,[19] and have not been detected experimentally so far. The second point is that the diiron frame seems flexible, from a stereochemical point of view, during the alkyne insertion. Thus, the final products may display both *cis* and *trans* configuration of the Cp ligands (see the specific cases in Scheme 2), while the starting complexes [**1a-b**]$^+$ are exclusively *cis*.[20,21] When observed, the *trans* product is a kinetic one, and can be quantitatively converted into the more stable *cis* counterpart upon thermal treatment. Moreover, E/Z isomery can be found in [**2**]$^+$, as a consequence of the two possible spatial orientations adopted by two different N-substituents (Scheme 2, inset).

Herein, we present the results of a DFT study to give insight into the mechanism of formation of [**2a-c**]$^+$ and to provide explanation for the stereochemistry exhibited by the products. Furthermore, [**2b-d**]SO_3CF_3 have been selected as starting materials for exploring new synthetic pathways to derivatize the vinyliminium ligand, resulting in unprecedented hydrocarbyl fragments.

Results and discussion

1. DFT and crystallographic studies.

First, the insertion reaction of propyne into the Fe-carbyne bond of [**1a**]$^+$ affording [**2a**]$^+$ [12a] was investigated (Scheme 3).

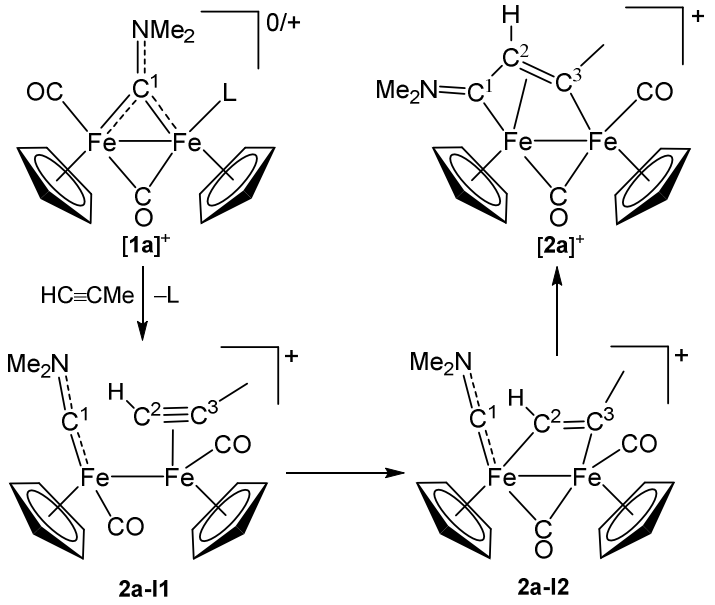

Scheme 3. Proposed DFT intermediates along the formation of [**2a**]$^+$ via propyne insertion into Fe-μ-carbyne bond (L = Cl or NCMe).

The alkyne is expected to initially coordinate one iron centre, although this modality has not been recognized experimentally. In the DFT-optimized geometry of **2a-I1** (Figure 1a), the bridging aminoalkylidyne is migrated to a terminal position, binding one single iron atom (Mayer bond orders [22] for Fe1-C1 and C1-N1 are 1.64 and 1.38, respectively). This rearrangement allows propyne to coordinate the other iron according to a slightly asymmetric η^2-mode (Fe2–C3 = 2.075 Å, Fe2–C4 = 2.101 Å). The two carbonyl ligands occupy terminal sites.

The possible intermediate **2a-I1** is 12.0 kcal mol^{-1} less table than **2a-I2**, wherein the alkyne bridges the two iron centers, and the conversion of the former into the latter requires a small activation energy ($\Delta G^{\ddagger}$ = 1.6 kcal mol^{-1}). In **2a-I2** (Figure 1b), the orientation of the alkyne Me-substituent minimizes steric repulsions and seems responsible for the observed regiospecificity of the process (see Introduction and Scheme 2). The distance between the alkyne carbon C2 and the carbyne C1 is 2.458 Å; this configuration is ideal for C1-C2 bond formation (*insertion reaction*) and **2a-TS2** has been

identified as the related transition state. In **2a-TS2**, the C1-C2 distance is shortened to 2.230 Å and the corresponding energy is only 0.4 kcal mol^{-1} higher than that of **2a-I2**.

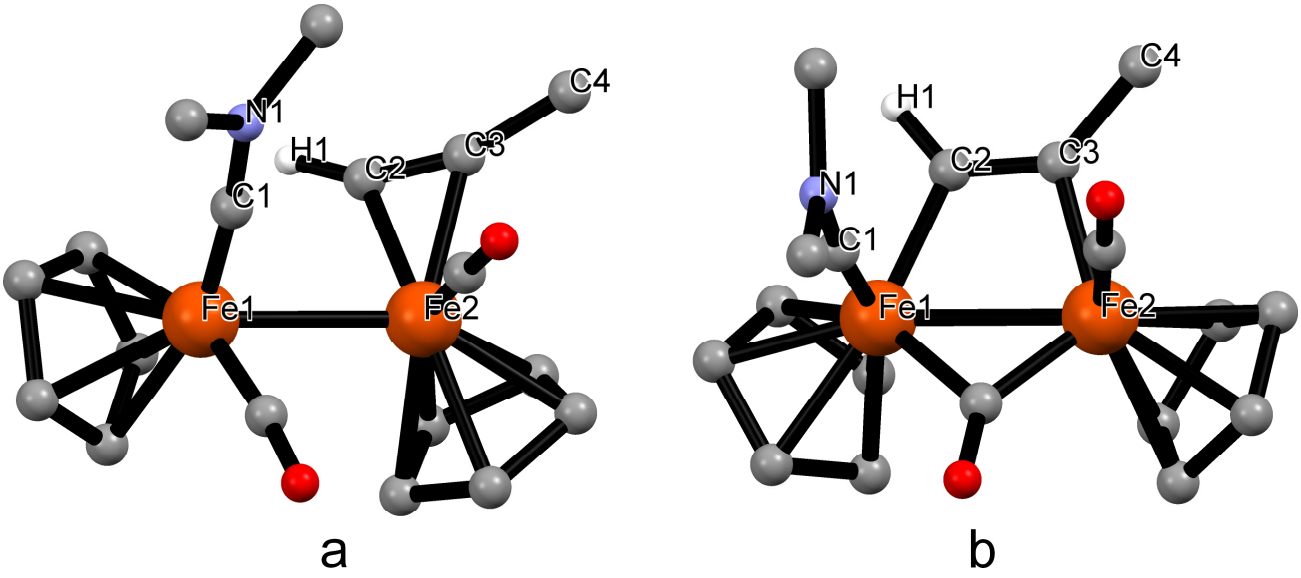

Figure 1. DFT-optimized geometries of **2a-I1** (a) and **2a-I2** (b). Hydrogen atoms (except H1) omitted for clarity. Selected distances (Å) and angles (°): **2a-I1** Fe1–Fe2 = 2.745, Fe1–C2 = 3.125, Fe2–C2 = 2.086, Fe2–C3 = 2.110, Fe2–C4 = 3.251, Fe1–C1 = 1.674, C1–N1 = 1.303, C1–C2 = 3.169, C2–C3 = 1.274, H1–C2–C3 = 151.8, C2–C3–C4 = 159.8, Fe1–C1–N1 = 172.9, C1–Fe1–Fe2–C2 = 72.6; **2a-I2** Fe1–Fe2 = 2.685, Fe1–C2 = 2.010, Fe2–C2 = 2.678, Fe2–C3 = 2.010, Fe1–C1 = 1.655, C1–N1 = 1.304, C1–C2 = 2.458, C2–C3 = 1.326, H1–C2–C3 = 128.6, C2–C3–C4 = 131.2, Fe1–C1–N1 = 173.6.

After insertion, the system collapses to the final product [**2a**]$^+$, being 47.8 kcal mol^{-1} more stable than **2a-I2** (a view of the calculated structure of [**2a**]$^+$ is shown in Figure S1). The structure of [**2a**]SO_3CF_3 was experimentally determined by X-ray diffraction: a view of the cation is given in Figure 2, while the salient bonding parameters are reported in Table 1, showing substantial agreement with the corresponding DFT data and with analogous structures previously reported but comprising a xylyl N-substituent.[12]

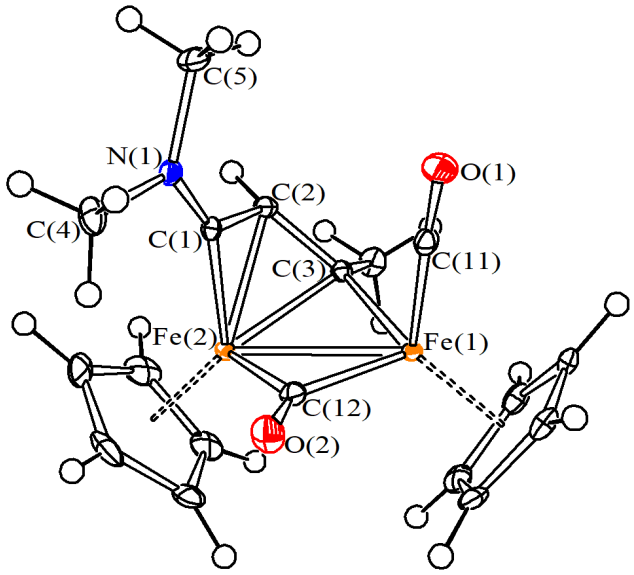

Figure 2. Molecular structure of [**2a**]$^+$ with key atoms labeled. Displacement ellipsoids are at the 30% probability level.

Table 1. Selected bond distances (Å) and angles (°) for [**2a**]$^+$ (experimental and calculated values).

	X-Ray	**DFT**
Fe(1)-Fe(2)	2.5535(3)	2.538
Fe(1)-C(11)	1.7689(17)	1.728
Fe(1)-C(12)	1.9116(17)	1.894
Fe(2)-C(12)	1.9305(17)	1.928
Fe(1)-C(3)	1.9565(16)	2.062
Fe(2)-C(3)	2.0414(16)	1.954
Fe(2)-C(1)	1.8550(16)	1.844
Fe(2)-C(2)	2.0628(16)	2.103
C(11)-O(1)	1.139(2)	1.194
C(12)-O(2)	1.176(2)	1.217
C(1)-C(2)	1.422(2)	1.448
C(2)-C(3)	1.415(2)	1.448
C(1)-N(1)	1.281(2)	1.317
N(1)-C(4)	1.470(2)	1.490
N(1)-C(5)	1.468(2)	1.493

Fe(1)-C(11)-O(1)	177.18(15)	179.01
Fe(1)-C(12)-Fe(2)	83.30(7)	83.24
Fe(1)-C(3)-Fe(2)	79.36(6)	78.37
Fe(1)-C(3)-C(2)	119.51(12)	120.38
C(3)-C(2)-C(1)	116.06(14)	113.27
C(2)-C(1)-N(1)	133.68(15)	133.78
C(2)-C(1)-Fe(2)	76.76(9)	78.40
C(1)-N(1)-C(4)	121.56(14)	121.56
C(1)-N(1)-C(5)	122.42(14)	122.88
C(4)-N(1)-C(5)	116.02(13)	115.48

It is interesting to note that, in [**2a**]$^+$ (Figure S1), the bonds C1-C2 and C2-C3 exhibit very similar lengths [calculated values: 1.448 (C1-C2) and 1.448 Å (C2-C3); X-ray values: 1.422(2) (C1-C2) and 1.415(2) Å (C2-C3)]. The Mayer bond orders for N-C1, C1-C2 and C2-C3 are 1.38, 1.12 and 1.05, respectively, confirming that the C_3 ligand can be well described as a vinyliminium, with the alkenyl moiety C2-C3 being elongated due to coordination to Fe1. The Mayer bond orders for C1-Fe1, C2-Fe1, C3-Fe1 and C3-Fe2 are 1.01, 0.38, 0.54 and 0.91, respectively.

The *trans* isomer of [**2a**]$^+$ (experimentally not observed [12a]) could be originated from **2a-I1**, by means of rotation around the Fe-Fe axis affording **2a-I1T** (**2a-I1T** is 30.1 kcal mol^{-1} more stable than **2a-I1**). The transition state for this rotation lies 11.9 kcal mol^{-1} higher than **2a-I1**, therefore it is expected to be accessible at ambient temperature (**2a-TS$_{cis\text{-}trans}$**). Indeed intramolecular ligand interchanges between cis/trans and bridging/terminal sites in related diiron systems were previously explained in a similar way (Adams-Cotton mechanism).[23] DFT calculations point that **2a-I1T** has a different geometry than **2a-I1**, in that the aminocarbyne bridging coordination is maintained after alkyne binding to one Fe atom (Figure 3a). Nevertheless, further rearrangement to **2a-I2T**, bearing a bridging alkyne (Figure 3b), appears necessary to allow the C1-C2 bond formation. However, the activation energy for the trans to cis isomerization is much higher than that requested for the formation of **2a-I1**, which makes the whole *trans* path unlikely. The *trans* isomer (Figure 3c) is not favored even on thermodynamic basis,

since it is 2.3 kcal mol^{-1} less stable than cis-[**2a**]$^{+}$. A comparative overview of the energy profiles of the calculated pathways leading to cis-[**2a**]$^{+}$ and trans-[**2a**]$^{+}$ is given in Figure 4.

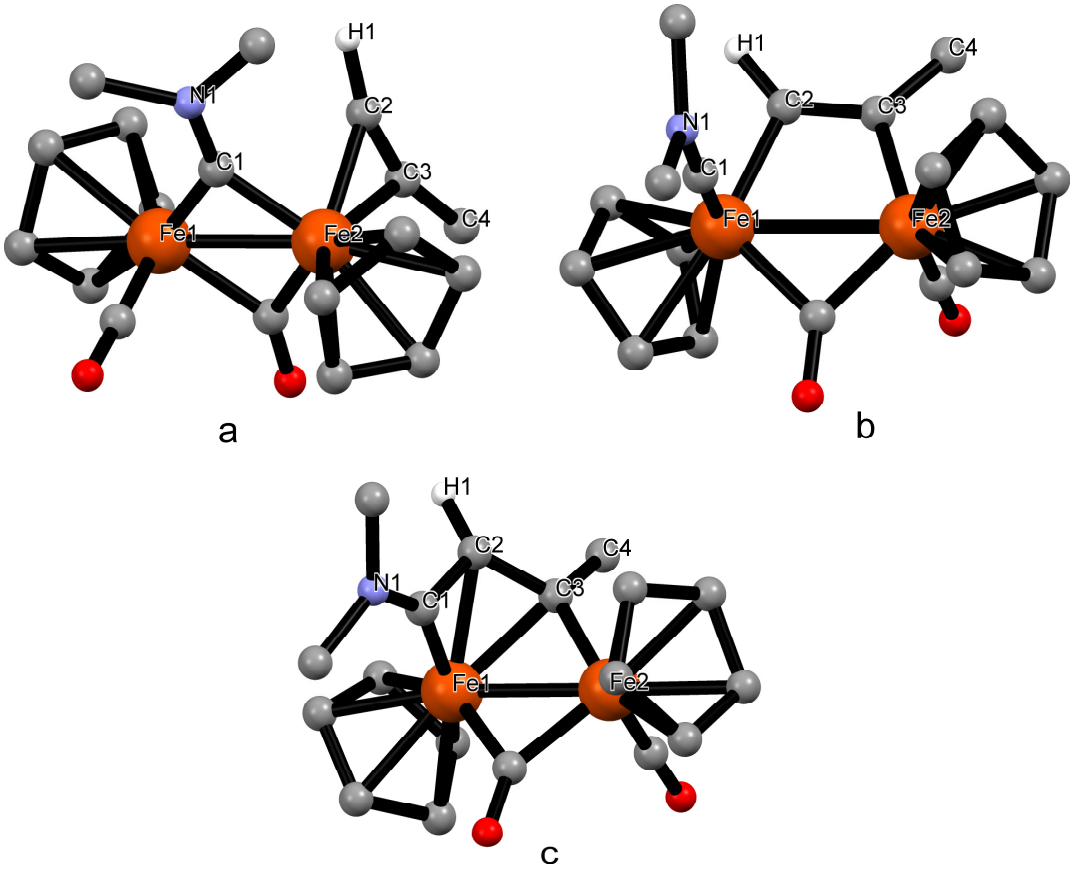

Figure 3. DFT-optimized geometries of **2a-l1T** (a), **2a-l2T** (b) and trans-[**2a**]$^{+}$ (c). Hydrogen atoms (except H1) omitted for clarity. Selected distances (Å) and angles (°): **2a-l1T** Fe1–Fe2 = 2.516, Fe1–C1 = 1.852, Fe2–C1 = 1.862, Fe2–C2 = 2.104, Fe2–C3 = 2.148, C1–N1 = 1.328, C2–C3 = 1.270, H1–C2–C3 = 153.5, C2–C3–C4 = 160.1, Fe1–C1–N1 = 136.7; **2a-l2T** Fe1–Fe2 = 2.685, Fe1–C1 = 1.649, C1-N1 = 1.309, Fe1–C2 = 2.008, Fe2–C3 = 2.014, Fe2-C2 = 2.663, C2–C3 = 1.321, H1–C2–C3 = 129.3, C2–C3–C4 = 131.9, Fe1–C1–N1 = 176.8; trans-[**2a**]$^{+}$ Fe1–Fe2 = 2.529, Fe1–C1 = 1.837, C1-N1 = 1.319, Fe1–C2 = 2.090, Fe1–C2 = 2.059, Fe2–C3 = 1.940, C1–C2 = 1.449, C2–C3 = 1.438, H1–C2–C3 = 121.5, C2–C3–C4 = 119.3, Fe1–C1–N1 = 147.5.

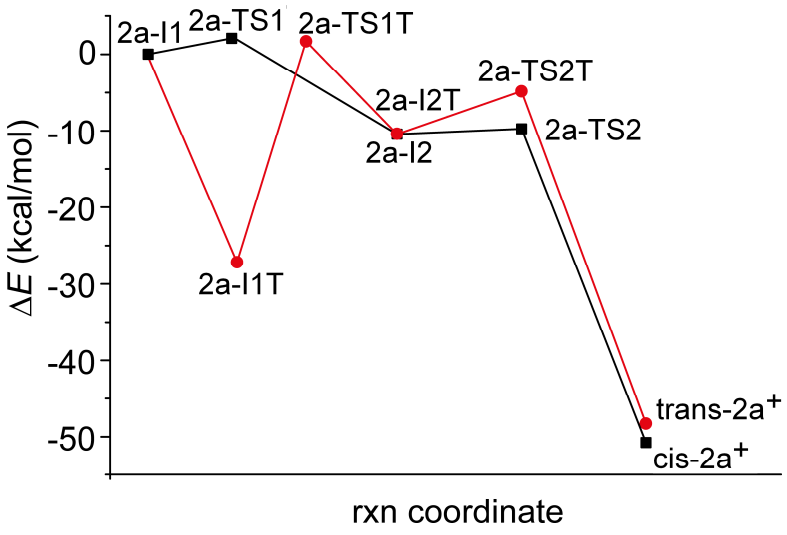

Figure 4. Energy profiles of the pathways leading to cis-[**2a**]$^+$ (black line) and trans-[**2a**]$^+$ (red line).

Trying to elucidate the synthesis of [**2b**]$^+$,[12a] the picture is qualitatively similar to what discussed for [**2a**]$^+$, but E and Z isomerism, beyond cis/trans, is also possible. Indeed the energy difference between (cis-E)-[**2b**]$^+$ and (cis-Z)-[**2b**]$^+$ is only 0.8 kcal mol^{-1}, thus justifying the formation of both forms (experimental E to Z ratio = 2). The obtained product exclusively displays cis geometry, which is more stable than the trans one by 1.8 kcal mol^{-1}. Views of the calculated structures of (cis-E)-[**2b**]$^+$ and (cis-Z)-[**2b**]$^+$ are provided as Supporting Information (Figure S2).

Regarding [**2c**]$^+$, the experimental outcome points out that the trans-Z isomer (Figure 5) is the kinetic product, converting into the cis-Z isomer by thermal treatment.[12b] DFT calculations show that the coordination of 2-butyne forces the aminoalkylidyne to shift to one single iron atom (**2c-I1**). This configuration is stabilized by a CH$\cdots\pi$ weak interaction between the aromatic ring of the xylyl moiety and the methyl belonging to the alkyne. Due to this interaction, which is lost in the TS, the activation barrier for the migration of the alkyne to bridging position (**2c-I2**, ΔG = –9.1 kcal mol^{-1}) is 12.6 kcal mol^{-1} (**2c-TS1**) i.e. higher respect to the case of [**2a**]$^+$. The subsequent insertion step leads to the cis-Z

isomer (ΔG(**2c-TS2**) = −7.5 kcal mol^{-1}; ΔG(cis-[**2c**]$^+$) = −47.2 kcal mol^{-1}). The route to the *trans* isomer is more probable: starting from **2c-I1**, the activation barrier for the rotation around the Fe-Fe bond is 9.9 kcal mol^{-1} (**2c-TS$_{cis-trans}$**), i.e. lower than the activation energy required by **2c-TS1**. The rotation leads to the *trans* isomer, **2c-I1T** (Figure 5), being 29.2 kcal mol^{-1} more stable than **2c-I1**. Then the alkyne can move to bridging position (ΔG(**2c-TS1**) = 4.7 kcal mol^{-1}; ΔG([**2c-I2T**]$^+$) = −4.8 kcal mol^{-1}, see Figure 5) and, finally, the insertion step takes place almost barrierless (ΔG(**2c-TS2**) = −7.7 kcal mol^{-1}), leading to the product (ΔG((cis-*Z*)-[**2c**]$^+$) = −53.6 kcal mol^{-1}), Figure 6. It is possible that the thermal isomerization of (trans-Z)-[**2c**]$^+$ to (cis-Z)-[**2c**]$^+$ [12b] proceeds through fast de-insertion of the alkyne, thus allowing the system to reach the thermodynamic equilibrium. The calculated structure of (cis-Z)-[**2c**]$^+$ is shown in Figure S4, while a comparison of calculated and experimental bonding parameters is given in Table S1.

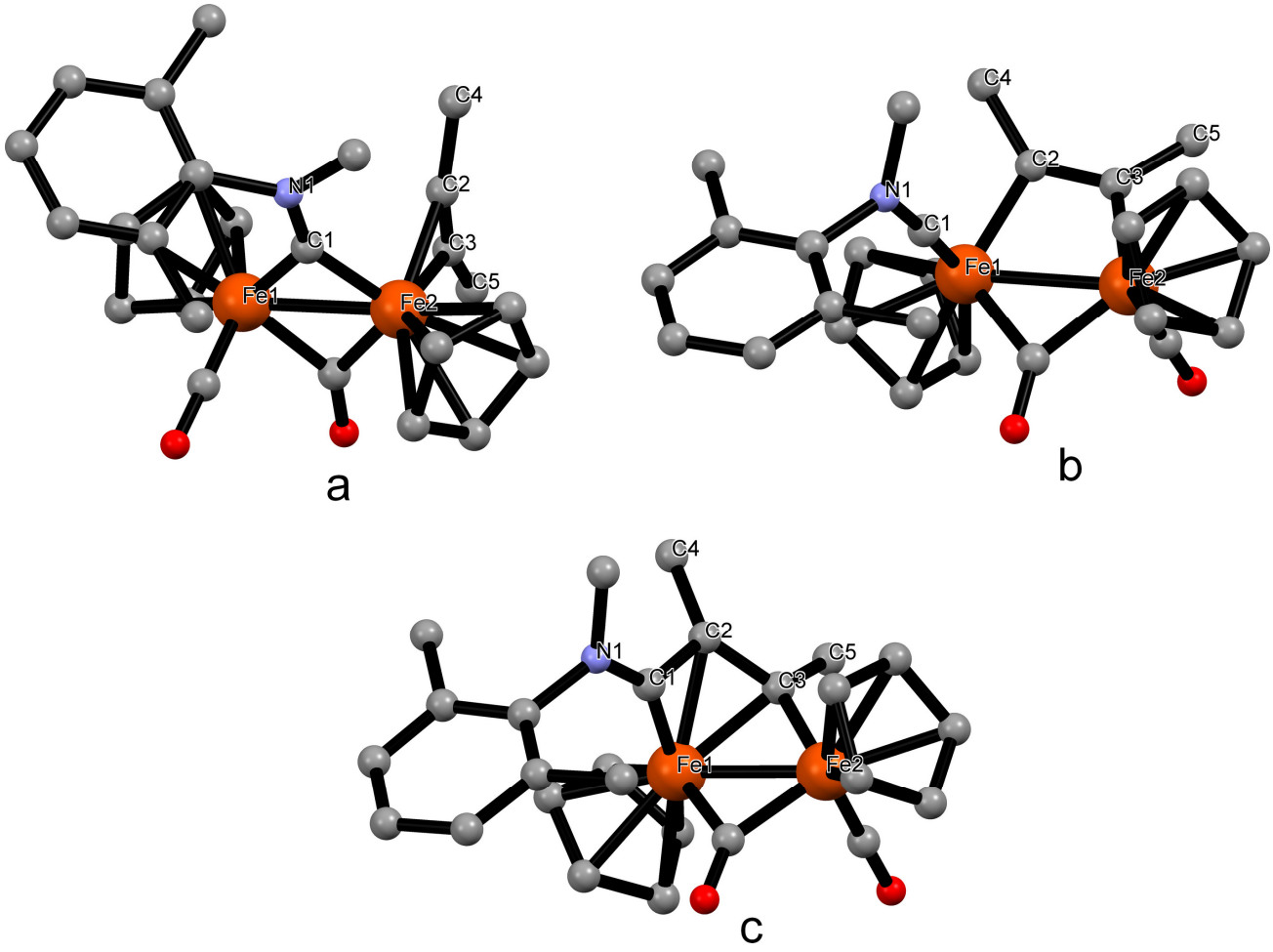

Figure 5. DFT-optimized geometries of **2c-l1T** (a), **2c-l2T** (b) and (trans-Z)-[**2c**]$^+$ (c). Hydrogen atoms omitted for clarity. Selected distances (Å) and angles (°): **2c-l1T** Fe1–Fe2 = 2.513, Fe1–C1 = 1.870, Fe2–C1 = 1.848, Fe2–C2 = 2.124, Fe2–C3 = 2.140, C1–N1 = 1.337, C1–C2 = 2.742, C2–C3 = 1.271, C2–C4 = 1.483, C4–C2–C3 = 153.0, C2–C3–C5 = 157.5, Fe1–C1–N1 = 134.6; **2c-l2T** Fe1–Fe2 = 2.651, Fe1–C1 = 1.644, Fe1–C2 = 2.018, Fe2–C2 = 2.703, Fe2–C3 = 2.606, C1–N1 = 1.310, C2–C3 = 1.324, C2–C4 = 1.511, C4–C2–C3 = 131.5, C2–C3–C5 = 130.6, Fe1–C1–N1 = 175.1; (trans-Z)-[**2c**]$^+$ Fe1–Fe2 = 2.531, Fe1–C1 = 1.337, Fe1–C2 = 2.123, Fe1–C3 = 2.034, Fe2–C3 = 1.938, C1–N1 = 1.326, C1–C2 = 1.452, C2–C3 = 1.444, C2–C4 = 1.526, C1–C2–C3 = 113.3, N1–C1–C2 = 132.2, C2–C3–C5 = 120.2.

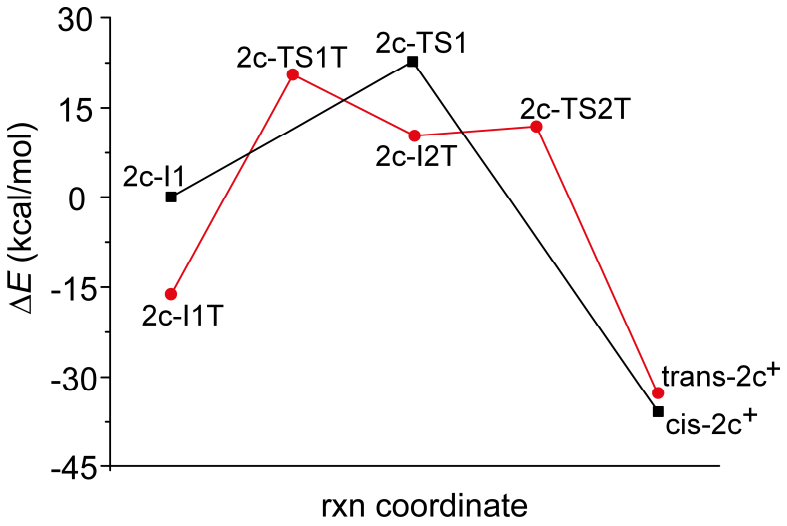

Figure 6. Energy profiles of the pathways leading to (cis-Z)-[**2c**]$^+$ (black line) and (trans-Z)-[**2c**]$^+$ (red line).

2. C-C coupling reactions.

The vinyliminium ligand is a useful substrate to generate C-C bonds, and previous reports regarded the addition of cyanide ion,[24] acetylides [25] and isocyanides.[26] We came interested in the possibility of tethering alkenes to the vinyliminium skeleton upon C^2-H removal. The investigation of the reactivity of [**2a-b**]SO_3CF_3 with a series of alkenes did not afford stable products, except in one case. Thus, the reaction of [**2b**]SO_3CF_3 with cyclopentene, in tetrahydrofuran in the presence of sodium hydride, afforded a modest amount of the fulvene-bis-alkylidene complex **3**, in admixture with other non identified species (Scheme 4).

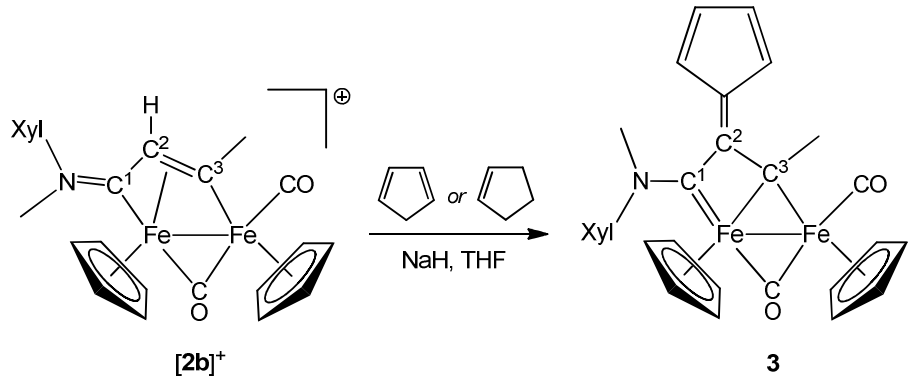

Scheme 4. Modification of a vinyliminium ligand with a fulvene moiety via unusual activation of cyclopentadiene/cyclopentene.

The formation of **3** is notable, since it requires a cycloalkene activation (from cyclopentene to fulvene) almost unknown in the literature. Compound **3** was purified by alumina chromatography and fully characterized by elemental analysis, mass spectrometry, IR and NMR spectroscopy. Once the structure of **3** had been elucidated, we evaluated that cyclopentadiene could be a more suitable reactant to the synthesis. As a matter of fact, **3** was obtained with an optimized yield of 61% from [**2b**]SO_3CF_3, freshly distilled cyclopentadiene and sodium hydride (Scheme 4). The formation of **3** appears the result of coupling of dehydrogenated cyclopentadiene with the deprotonated form of [**2b**]$^+$, possessing some carbene character (Figure 7).[26] It should be mentioned here that the uncommon cyclopentadiene to fulvene conversion was previously reported upon base-assisted condensation with ketones,[27] but it is unprecedented for an organometallic structure.

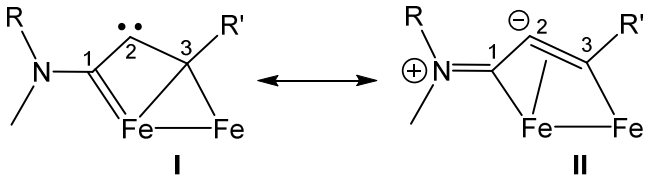

Figure 7. Resonance forms representing the fragment derived from vinyliminium C^2-H deprotonation.

The IR spectrum of **3** (in CH_2Cl_2 solution) displays two bands due to the carbonyl ligands (at 1949 and 1783 cm^{-1}), and an additional absorption at 1551 cm^{-1}, assigned to the coupled vibrations of the C^1=N and the C^2=C^3 bonds by comparison with the calculated IR spectrum (vide infra). The ^{1}H NMR spectrum (in $CDCl_3$) contains one set of resonances, and the signals related to the fulvene moiety consist of two multiplets at 6.49 and 6.36 ppm, thus indicating free rotation at ambient temperature around the C^2-C bond (vide infra). A NOE experiment by irradiating the Cp resonance at 4.35 ppm

resulted in a significant enhancement of the remaining Cp signal at 4.97 ppm, pointing that the two rings are arranged in relative *cis* geometry. On the other hand, irradiation of the resonance at 3.27 ppm (NMe) revealed NOE effect with the CH fulvene resonance at 6.49 ppm, but not with any Cp resonance. This outcome clearly indicates that the N-bound methyl group points far from the Fe-Fe axis, the same Z-configuration being usually adopted by diiron complexes comprising C^2-substituted vinyliminium and bis-alkylidene ligands.[16a,12b,28]

The ^{13}C resonances related to the C^1 and C^3 carbons fall at typical low fields (247.4 and 195.1 ppm), in agreement with their amino-alkylidene and alkylidene character, respectively.[15b]

Several attempts were done to collect X-ray quality crystals of **3**, but unsuccessfully. The structure of **3** (in the cis-Z form, as indicated by NMR) was therefore optimized by DFT calculations, and a view of the structure is shown in Figure 8 with calculated bonding parameters reported in the caption.

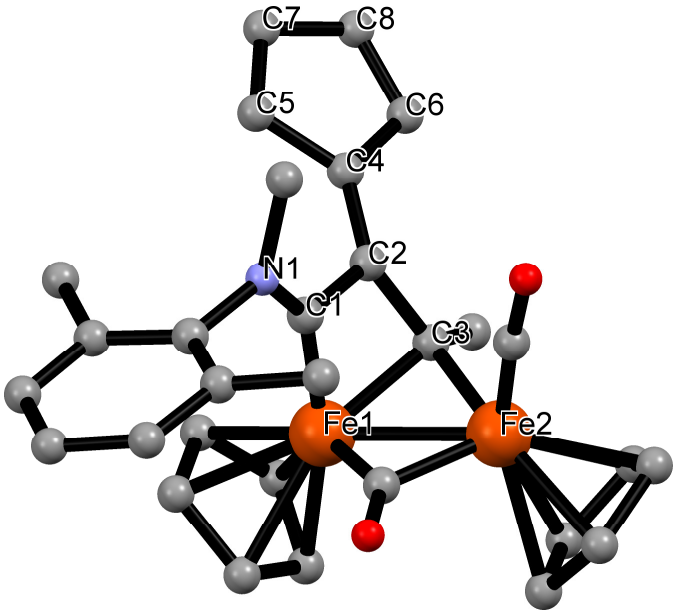

Figure 8. DFT-optimized geometry of **3**. Hydrogen atoms omitted for clarity. Selected bond lengths (Å) and angles (°): Fe1–Fe2 = 2.503, Fe1–C1 = 1.865, Fe1–C3 = 2.014, Fe1–C2 = 2.403, Fe2–C3 = 1.981, C1–C2 = 1.477, C2–C3 = 1.486, C1–N1 = 1.339, C2–C4 = 1.414, C4–C5 = 1.472, C5–C7 = 1.389, C7–C8 = 1.470, C6–C8 = 1.390, C6–C4= 1.472, C1–C2–C3= 102.5, C2–C1–N1= 127.7, C1–C2–C6 = 125.0, N1-C1-C2-C4 = -48.1.

The Mayer bond orders for N1-C1, C1-C2, C2-C3 and C2-C4 are 1.36, 0.97, 0.83 and 1.24, respectively (the calculated C2-C4 bond length is 1.414 Å). The DFT data suggest some zwitterionic character in the structure of **3**, whose bridging C_3 ligand should be alternatively described as a vinyliminium with the negative charge delocalized on the five-membered substituent (Figure 9). Analogous vinyliminium/bis-alkylidene hybrid structure was revealed by the crystallographic characterization of $[Fe_2Cp_2(CO)(\mu\text{-}CO)\{\mu\text{-}\eta^1\text{:}\eta^2\text{-}C(Me)C(O)CN(Me)(Xyl)\}]$, differing from **3** in the presence of an oxygen atom in the place of the fulvene moiety.[28] It has to be remarked that the latter two complexes exhibit very close IR spectra and comparable values of ^{13}C NMR chemical shifts for C^1 and C^3.[29] Structure **II** in Figure 9 accounts for the experimentally observed free rotation of the C_5 ring around the C2-C4 bond at ambient temperature (see above).

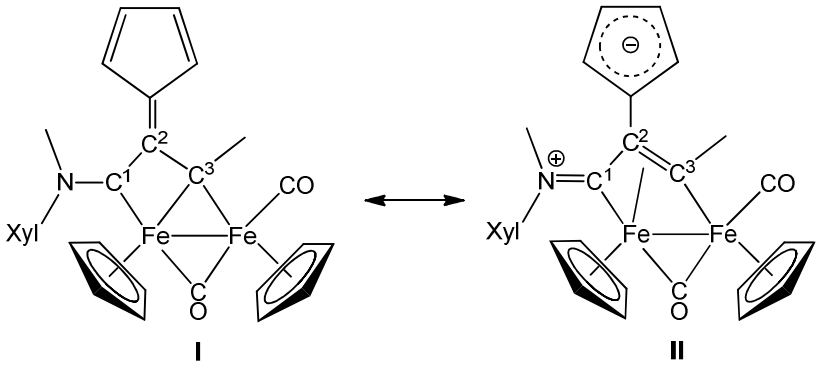

Figure 9. Resonance formulas describing the structure of **3** (compare to Figure 7).

The reaction of [**2b**]SO_3CF_3 with $PPh_3{=}CH_2$/NaH, in tetrahydrofuran, readily proceeded with the clean formation of a neutral product, as suggested by the IR spectrum recorded on the reaction solution after 30 minutes [ν_{CO} = 1952 and 1773 cm^{-1}]. It is reasonable to assume that the detected compound is the bis-alkylidene **4**, analogous to **3** (Figure 9, structure **I**). The formation of **4** might be viewed as the coupling between the carbene moiety belonging to deprotonated $[\mathbf{2b}]^+$ (Figure 7, structure **I**) and the $[CH_2]$ fragment originating from $PPh_3{=}CH_2$. Examples of $[CH_2]$ transfer from $Ph_3P{=}CH_2$ to carbene groups were indeed previously documented.[30] Attempts to isolate **4** were unsuccessful, and led to

recovery of a small amount of [**2b**]SO_3CF_3. Instead, the treatment of the reaction mixture with HSO_3CF_3 resulted in the fast and clean formation of [**2c**]SO_3CF_3 (Scheme 5), which was isolated in 75% yield after work up, and unambiguously identified by elemental analysis, IR and ^{1}H NMR spectroscopy.

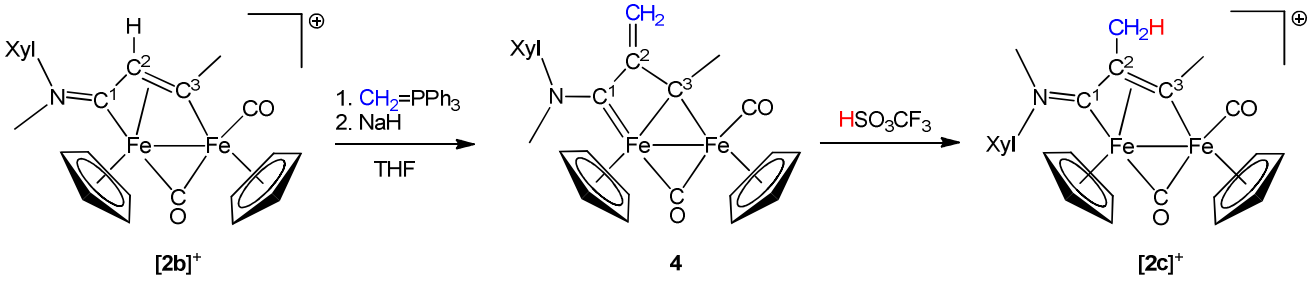

Scheme 5. Two-step H^+-CH_3^+ substitution at a vinyliminium ligand.

The structure of **4** was optimized by DFT calculations; the calculated bonding parameters are in well agreement with a bis-alkylidene nature of the bridging C_3 ligand [15b] (Figure 10). On theoretical grounds, the E isomer is slightly more stable than the opposite Z one (ΔE = 2.0 kcal mol^{-1}), presumably due to attractive forces between the [CH_2] group and the aromatic xylyl ring (CH - π interaction). However, the final product [**2c**]$^+$ was recognized in the *Z* form (Scheme 2). This fact indicates that *E* to *Z* conversion must take place on going from [**2b**]$^+$ to [**2c**]$^+$ via **4**, possibly through rotation around the C^1–N axis in **4** (calculated C^1–N distance = 1.346 Å).

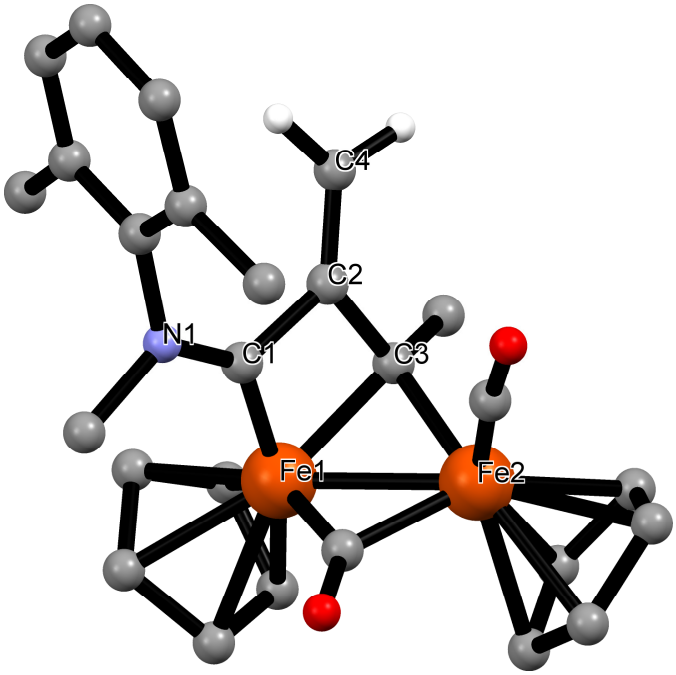

Figure 10. DFT-optimized geometry of E-**4**. Hydrogen atoms (except CH_2) omitted for clarity. Selected bond lengths (Å) and angles (°): Fe1-Fe2 = 2.487, Fe1-C1 = 1.857, Fe1-C2 = 2.514, Fe1-C3 = 1.980, C1-N1 = 1.346, C1-C2 = 1.486, C2-C3 = 1.504, C2-C4 = 1.370, Fe2-C3 = 1.990, C1-C2-C3 = 98.3, C2-C1-N1 = 127.4, C3-C2-C6 = 128.5, N1-C1-C2-C4 = -17.9.

With the aim of further exploring the possibility of C-C bond formation, we studied the reaction of [**2b**]SO_3CF_3 with benzyl bromide, in the presence of sodium hydride. This reaction afforded the vinyliminium compound [**5**]Br in 55% yield, Scheme 6.

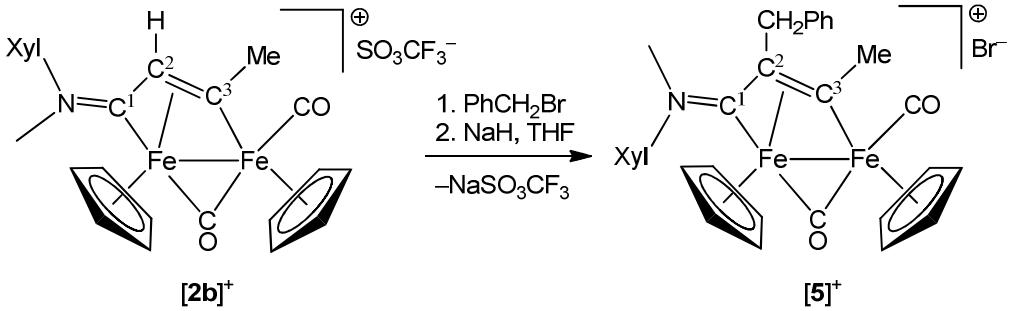

Scheme 6. Derivatization of vinyliminium ligand via C-H cleavage and C-C coupling.

Compound [**5**]Br was purified by quick chromatography through alumina, and then characterized by elemental analysis, IR and NMR spectroscopy. The IR spectrum (in CH_2Cl_2) displays a pattern

matching that of analogous complexes bearing alkyl substituents at both C^2 and C^3.[12b] More precisely, the two carbonyl bands are seen at 1986 and 1814 cm^{-1}, while the absorption due to the NC^1C^2 moiety falls at 1603 cm^{-1} [as a comparison, the corresponding values for (cis-Z)-[**2c**]SO_3CF_3 are: 1986, 1818 and 1613 cm^{-1} [12b]].

The NMR spectra of [**5**]Br (in $CDCl_3$) evidenced the presence of an isomeric mixture. In general, E/Z and cis/trans isomers of diiron vinyliminium complexes can be easily distinguished by ^1H and ^{13}C NMR data (especially the resonances due to Cp and methyl groups).[12] Therefore, in this case the isomers were identified as cis-E and cis-Z (E to Z ratio = 2, based on ^1H NMR). The ^{19}F spectrum ruled out the presence of residual triflate anion.

In order to give insight into thermodynamic and structural aspects, we calculated the structures of E-[**5**]$^+$ and Z-[**5**]$^+$ (Figure 11). The *Z* isomer resulted 2.0 kcal mol^{-1} more stable than the *E* one. In accordance with the DFT outcome, the isomeric mixture was cleanly converted into the most stable Z form by heating in methanol solution.

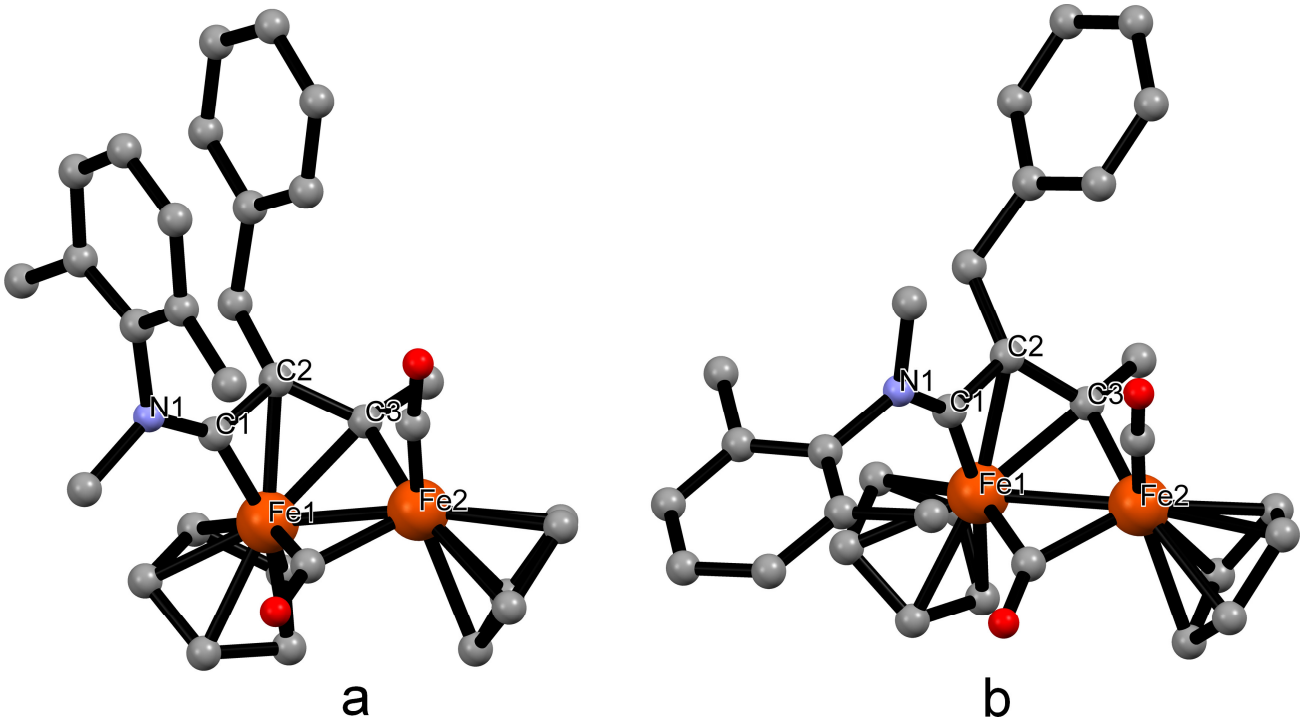

Figure 11. DFT-optimized geometries of (cis-E)-[**5**]$^+$ (a) and (cis-Z)-[**5**]$^+$ (b). Hydrogen atoms omitted for clarity. Selected distances (Å) and angles (°):(cis-E)-[**5**]$^+$ Fe1–Fe2 = 2.529, Fe1–C1 = 1.845, Fe1–C2 = 2.098, Fe1–C3 = 2.048, Fe2–C3 = 1.952, C1–N1 = 1.322, C1–C2 = 1.447, C2–C3 = 1.452, C1–C2–C3 = 144.5, Fe1–C1–N1 = 144.9; (cis-Z)-[**5**]$^+$ Fe1–Fe2 = 2.543, Fe1–C1 = 1.849, Fe1–C2 = 2.104, Fe1–C3 = 2.063, Fe2–C3 = 1.945, C1–N1 = 1.320, C1–C2 = 1.445, C2–C3 = 1.446, C1–C2–C3 = 114.6, Fe1–C1–N1 = 148.3.

The synthesis of [**5**]$^+$ is formally the result of deprotonation of the parent vinyliminium followed by nucleophilic attack of the resulting zwitterionic species (Figure 7, structure **II**) to the alkyl halide. Despite the tendency of benzyl bromide to be engaged in radical reactions,[31] the possibility of an alternative, radical pathway starting with the NaH-reduction of [**2b**]$^+$ should be ruled out: as a matter of fact, the reaction of [**2b**]SO_3CF_3 with benzyl bromide in the presence of cobaltocene, i.e. a typical mono electron reductant employed in organometallic chemistry,[32] resulted in the formation of a mixture of products not including [**5**]$^+$.

3. Synthesis of thiophenolate compounds.

The chemistry of the vinyliminium compounds [**2c-d**]SO_3CF_3 is limited by the absence of C^2-bound hydrogen, not allowing the structural modifications otherwise described for [**2a-b**]$^+$ (Schemes 4-6). Notwithstanding, it has been documented that C^2-substituted vinyliminium compounds may convert into mono-iron species leaving the C^1-C^2-C^3 chain intact, upon reaction with strong reducing agents (NaH or Li^{t}Bu).[33] Sulfur or selenium can be incorporated during the fragmentation process, leading to functionalized metallacycles.[18]

We studied the reactivity of [**2c-d**]SO_3CF_3 with NaH in the presence of PhSSPh. The reaction involving [**2c**]$^+$ proceeded with alkyne de-insertion and binding of the [SPh] group to one metal center, affording the μ-aminocarbyne complex [Fe_2Cp_2(SPh)(CO)(μ-CO){μ-CN(Me)(Xyl)}], **6**, in 68% yield (Scheme 7a and Figure 12a). The aminocarbyne moiety manifests itself with a diagnostic ^{13}C NMR resonance at characteristic low field (338.5 ppm, $CDCl_3$ solution).[20,34] The IR and NMR features of **6** match those of similar diiron μ-aminocarbyne complexes with *cis*-oriented Cp ligands.[34f-g,35]

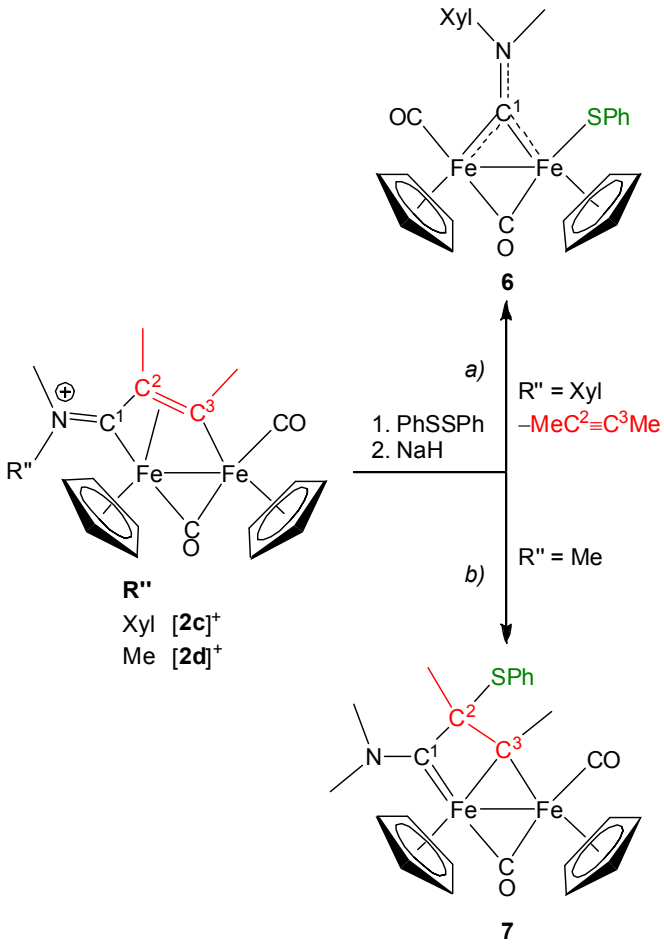

Scheme 7. Reactions of vinyliminium complexes with diphenyldisulphide in the presence of sodium hydride: a) de-insertion reaction; b) formation of [SPh]-functionalized bridging ligand.

Interestingly, the reaction of [**2d**]SO_3CF_3 with PhSSPh/NaH revealed a completely different outcome, and afforded the bis-alkylidene product $[Fe_2Cp_2(CO)(\mu\text{-}CO)\{\mu\text{-}\eta^1\text{:}\eta^2\text{-}C(Me)C(Me)(SPh)CN(Me)_2\}]$, **7**, in 55% yield (Scheme 7b and Figure 12b).

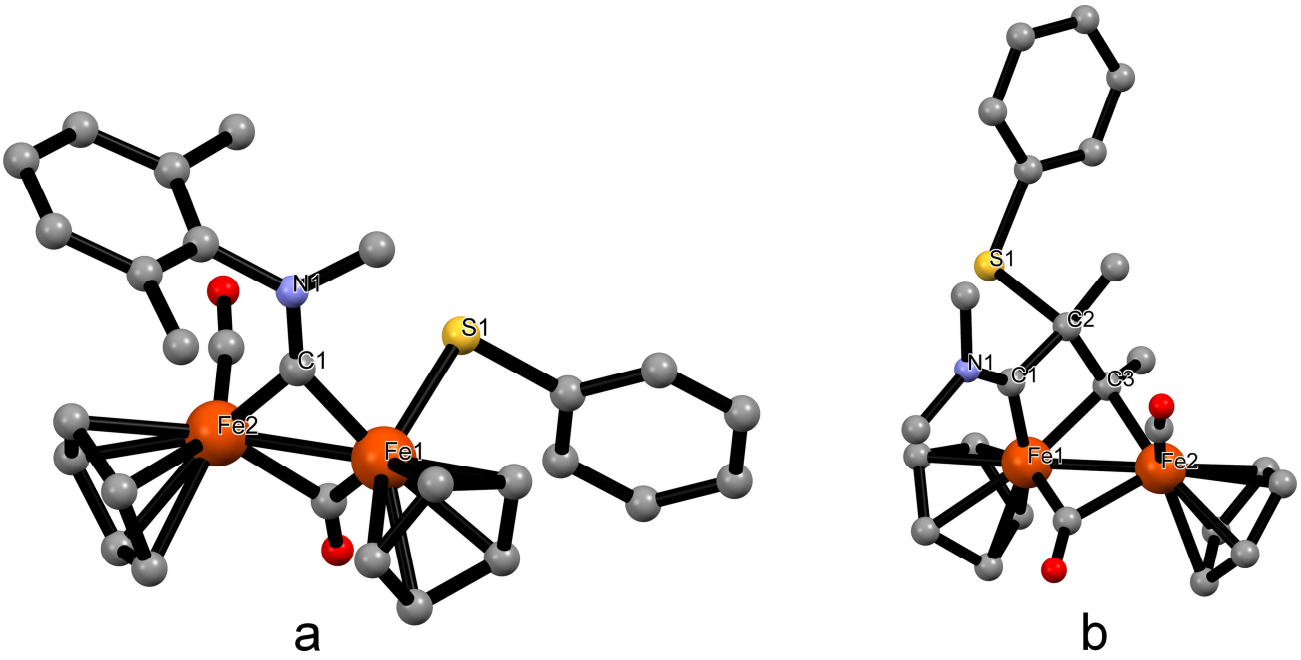

Figure 12. DFT-optimized structures of **6** (a) and **7** (b). Hydrogen atoms omitted for clarity. Selected distances (Å) and angles (°): **6** Fe1-Fe2 = 2.473, Fe1-C1 = 1.861, Fe2-C1 = 1.807, C1-N1 = 1.338, Fe2-S1 = 2.371, Fe1–C1–N1 = 137.0, C1–Fe2–S = 85.4, Fe2–S1–C3 = 104.1; **7** Fe1-Fe2 = 2.484, Fe1-C1 = 1.868, Fe1-C2 = 2.559, Fe1-C3 = 1.957, Fe2-C1 = 3.072, Fe2-C3 = 2.022, C1-C2 = 1.526, C2-C3 = 1.528, C2-S1 = 2.108, C1-N1 = 1.337, Fe1–C1–N1 = 136.8, C1–C2–C3 = 94.4, C1–C2–S1 = 97.8.

The IR spectrum of **7** displays carbonyl bands at typically low wavenumbers (1929 and 1752 cm^{-1}), as already found for other diiron complexes containing the bis-alkylidene skeleton.[15b] In the ^{1}H NMR spectrum, the Cp ligands resonate at 4.61 and 4.39 ppm, these values indicating a *cis* arrangement by comparison with a library of data referring to analogous compounds.[15b] The major NMR features are given by the low field ^{13}C resonances at 251.6 and 177.0 ppm, attributed to the alkylidene carbons C^{1} and C^{3}, respectively. In accordance with the aminocarbene character of C^{1}, the two N-bound methyl groups are not equivalent due to inhibited rotation around the N-C^{1} bond.

The distinct outcomes of the reactions of the homologous vinyliminium salts [**2c-d**]SO_3CF_3 with PhSSPh/NaH were investigated by DFT calculations. It is reasonable to assume that both reactions proceed with initial electron transfer from sodium hydride to the cationic complexes [**2c-d**]$^{+}$ to give **2c-d**, and subsequent capture of the thiophenolato radical by **2c-d**. On the other hand, the nucleophilic attack to [**2c-d**]$^{+}$ of the thiophenolate anion, this anion possibly generated from the interaction of

diphenyldisulphide with sodium hydride, was ruled out on the basis of the experimental evidence that the reactions of [**2c-d**]SO_3CF_3 with 1-2 equivalents of NaSPh in tetrahydrofuran did not produce **6-7**. More precisely, [**2d**]SO_3CF_3 revealed to be substantially unreactive, while the addition of NaSPh to [**2c**]SO_3CF_3 led to a mixture of decomposition products. The structures of the radical species **2c-d** were optimized by DFT (doublet state), resulting rather similar to those of the corresponding parent complexes [**2c-d**]$^+$. However, a slight lengthening of the C1-N bond is observable on going from [**2c-d**]$^+$ to **2c-d** (from 1.317 to 1.337 Å; Mayer bond order from 1.38 to 1.21). The spin density maps related to **2c-d** are shown in Figure 13: in both compounds, the spin density has a significant component on the bridging ligand (see Table S2 for details). This favors the SPh attack to the C^2 carbon of **2d** to give **7**. On the other hand, the major steric hindrance exerted by the iminium group in **2c** is presumably responsible for addressing the SPh addition to iron, to give **6**.

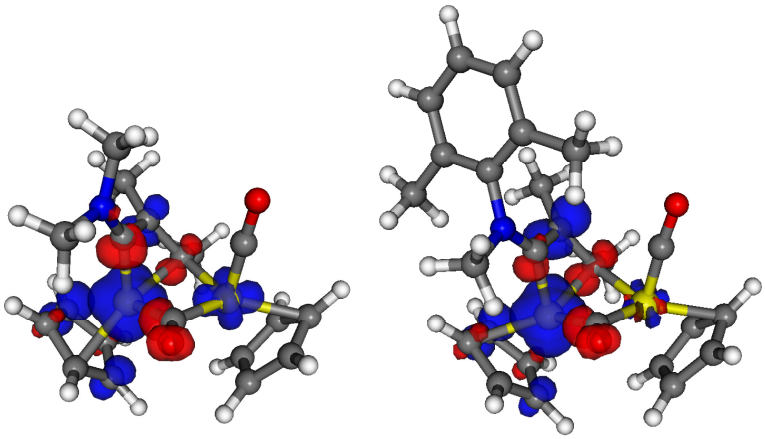

Figure 13. Spin density maps for radical complexes **2c** and **2d**.

Conclusions

Vinyliminium ligands in diiron complexes exhibit a rare bridging coordination fashion and a unique reactivity associated to the cooperative effects provided by the two iron centers and the net cationic charge of the compounds. Herein, we have proposed, based on DFT calculations, a mechanistic

pathway for the alkyne insertion implicated in the synthesis of the vinyliminium complexes. The described mechanism is in accordance with the regiospecificity of the reaction and the stereochemistry exhibited by the products (cis/trans and E/Z), depending on the iminium substituents and the alkyne. These findings may have some general validity, and might be extended to analogous alkyne insertion reactions occurring on dimetal frames.[3,9,10,11] Furthermore, we have described the synthesis of unprecedented organometallic motifs via vinyliminium C-H bond cleavage and subsequent C-C coupling with a variety of organic reactants, including the unusual activation of a cycloalkene. Vinyliminium complexes lacking of appropriate C-H function may be derivatized through one-electron reduction, the resulting radical species incorporating the [SPh] fragment in different ways according to the iminium substituents.

Experimental

Materials and methods. All the reactions were routinely carried out under nitrogen atmosphere, using standard Schlenk techniques. Organic reactants (Sigma Aldrich or TCI Europe) were commercial products of the highest purity available. Compounds [**1a-b**]SO_3CF_3,[20] triphenylphosphonium methylide (from methyltriphenylphosphonium bromide and LiBu),[36] and [**2c-d**]SO_3CF_3 [12b] were prepared according to published procedures. Solvents were distilled before use under nitrogen over appropriate drying agents. Once isolated, the metal products were conserved under nitrogen. Chromatography separations were carried out on columns of deactivated alumina (Sigma Aldrich, 4% *w/w* water). C, H, N analyses were performed on a ThermoQuest Flash 1112 Series EA Instrument. The bromide content of [**5**]Br was determined by the Mohr method [37] on a solution prepared by dissolution of the solid in aqueous KOH at boiling temperature, followed by cooling to room temperature and addition of HNO_3 up to neutralization. ESI-MS spectrum was recorded on Waters Micromass ZQ 4000 with the sample dissolved in CH_3CN. Infrared spectra were recorded on liquid samples with a Perkin-Elmer Spectrum

2000 FT-IR spectrophotometer. NMR spectra were recorded at 298 K on a Mercury Plus 400 instrument. The chemical shifts for ^{1}H and ^{13}C were referenced to the non-deuterated aliquot of the solvent. The ^{1}H and ^{13}C NMR spectra were assigned with the assistance of $^{1}H,^{13}C$ correlation measured through *gs*-HSQC and *gs*-HMBC experiments.[38] NMR signals due to a second isomeric form (where it has been possible to detect them) are italicized. NOE measurements were recorded using the DPFGSE-NOE sequence.[21]

Synthesis of $[Fe_2Cp_2(CO)(\mu\text{-}CO)\{\mu\text{-}\eta^1\text{:}\eta^3\text{-}C^3(Me)C^2HC^1N(Me)(R)\}]SO_3CF_3$ (R = Me, $[2a]SO_3CF_3$, Chart 1; R = Xyl, $[2b]SO_3CF_3$, Chart 2). The title compounds were prepared by using a modified literature procedure.[12b]

Chart 1. Structure of [**2a**]$^{+}$.

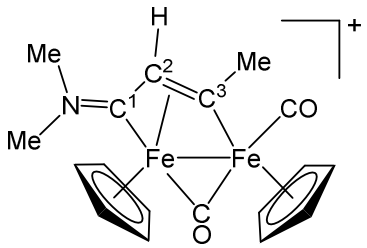

A solution of [**1a**]SO_3CF_3 (460 mg, 0.866 mmol) in acetonitrile (ca. 10 mL) was treated with Me_3NO (85 mg, 1.13 mmol). The solution turned darker and was stirred at room temperature for 40 min, allowing continuous flux of the produced gas (CO_2) away from the reaction system. Thus, IR spectroscopy indicated the complete conversion of the starting material into $[Fe_2Cp_2(CO)(\mu\text{-}CO)(NCMe)\{\mu\text{-}CNMe_2\}]SO_3CF_3$.[20] The volatiles were removed under vacuum. The residue was dissolved in CH_2Cl_2 (20 mL) and a solution of propyne in THF (3.5 mL, ca. 1 mol/L) was added. The resulting mixture was allowed to stir at room temperature for 72 h, then it was charged on an alumina column. After washings with CH_2Cl_2/THF (up to 2:1 v/v) mixtures, the product was collected as a brown fraction using neat MeOH as eluent. A brown solid was obtained upon removal of the solvent

under reduced pressure. Yield 451 mg, 96%. Anal. calcd. for $C_{19}H_{20}F_3Fe_2NO_5S$: C, 42.02; H, 3.71; N, 2.58. Found: C, 41.89; H, 3.64; N, 2.68. IR (CH_2Cl_2): $\tilde{\upsilon}$/cm^{-1} = 1990vs (CO), 1806s (μ-CO), 1684m (C^2C^1N). ^{1}H NMR (dmso-d_6): δ/ppm = 5.48, 5.14 (s, 10 H, Cp); 4.51 (s, 1 H, C^2H); 3.82, 3.77 (s, 6 H, NMe + C^3Me); 3.18 (s, 6 H, NMe). $^{13}C\{^1H\}$ NMR (dmso-d_6): δ/ppm = 258.4 (μ-CO); 225.6 (C^1); 211.4 (CO); 208.0 (C^3); 91.2, 88.0 (Cp); 52.1 (C^2); 51.0, 44.8 (NMe_2); 41.7 (C^3Me). Crystals suitable for X-ray analysis were obtained by slow diffusion of diethyl ether into a dichloromethane solution of [**2a**]SO_3CF_3 at ambient temperature.

Chart 2. Structure of [**2b**]$^+$.

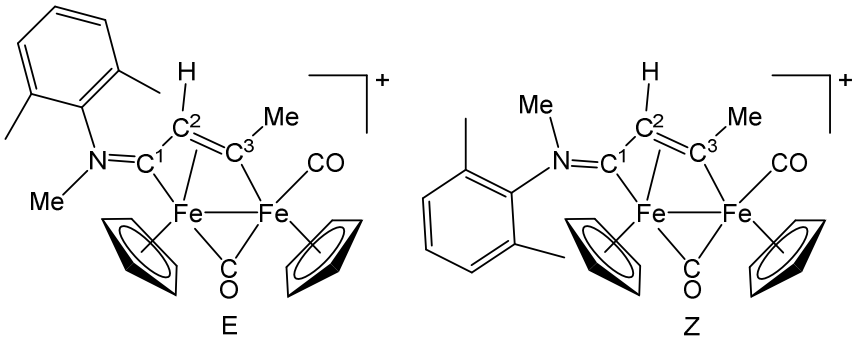

Compound [**2b**]SO_3CF_3 was obtained using the same procedure employed for the synthesis of [**2a**]SO_3CF_3, from [**1b**]SO_3CF_3 (450 mg, 0.724 mmol) and an excess of propyne. Yield 390 mg, 85%. Anal. Calcd. for $C_{26}H_{26}F_3Fe_2NO_5S$: C, 49.31; H, 4.14; N, 2.21. Found: C, 49.20; H, 4.22; N, 2.16. IR (CH_2Cl_2): ν/cm^{-1} = 2000vs (CO), 1815s (μ-CO), 1632m (NC^1C^2). ^{1}H NMR ($CDCl_3$): δ/ppm = 7.42-7.09, 6.92 (m, 3 H, $C_6H_3Me_2$); 5.39, *5.28*, 5.16, *4.72* (s, 10 H, Cp); *5.23*, 3.99 (s, 1 H, C^2H); 4.16, *3.48* (s, 3 H, NMe); *3.99*, 3.82 (s, 3 H, C^3Me); *2.53*, 2.28, *1.96*, 1.75 (s, 6 H, $C_6H_3Me_2$). E/Z ratio ≅ 2. $^{13}C\{^1H\}$ NMR ($CDCl_3$): δ/ppm = 254.6 (μ-CO); 233.4, *230.9* (C^1); 211.6, 211.4 (C^3); 210.6, 209.7 (CO); 144.8, *141.1* (*ipso*-$C_6H_3Me_2$); 134.0, 133.7, 131.6, 129.6, 129.5, 129.3, 129.0 ($C_6H_3Me_2$); 91.0, *90.7*, 87.8, *87.6* (Cp); *53.5*, 52.7 (C^2); *52.1*, 46.0 (NMe); 42.7, *42.3* (C^3Me); 17.9, 17.8, *17.7*, 17.2 ($C_6H_3Me_2$).

Synthesis of [$Fe_2Cp_2(CO)(\mu\text{-}CO)\{\mu\text{-}\eta^1\text{:}\eta^2\text{-}C^3(Me)C^2\{C(CH)_4\}C^1N(Me)(Xyl)\}$], 3 (Chart 3).

Chart 3. Structure of **3**.

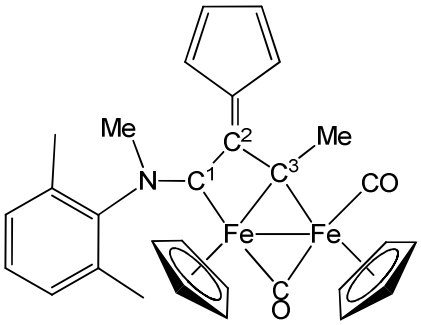

A solution of [**2b**]SO_3CF_3 (200 mg, 0.316 mmol) in THF (20 mL) was treated with freshly distilled cyclopentadiene (CpH; 0.18 mL, 2.1 mmol) and then with NaH (23 mg, 0.96 mmol). The resulting mixture was left stirring for 2 hours. The final mixture was filtered on a short alumina pad using THF as eluent, then the volatiles were removed under vacuum. The residue was dissolved in CH_2Cl_2 and charged on an alumina column; after washing with dichloromethane, a dark grey fraction corresponding to **3** was collected using neat THF as eluent. Yield 105 mg, 61%. Anal. Calcd. for $C_{30}H_{29}Fe_2NO_2$: C, 65.84; H, 5.34; N, 2.56. Found: C, 65.61; H, 5.40; N, 2.49. IR (CH_2Cl_2): ν/cm^{-1} = 1949vs (CO), 1783s (μ-CO), 1551m (C^1N + $C^2{=}C^3$) ^1H NMR ($CDCl_3$): δ/ppm = 7.37-7.22 (3 H, $C_6H_3Me_2$); 6.49, 6.36 (dd, 4 H, CH); 4.97, 4.35 (s, 10 H, Cp); 4.23 (s, 3 H, C^3Me); 3.27 (s, 3 H, NMe); 2.71, 2.09 (s, 6 H, $C_6H_3\mathit{Me}_2$). $^{13}C\{^1H\}$ NMR ($CDCl_3$): δ/ppm = 267.2 (μ-CO); 247.4 (C^1); 213.7 (CO); 195.1 (C^3); 142.0 (*ipso*-$C_6H_3Me_2$); 134.9, 134.2, 129.6, 128.8, 128.4 ($C_6H_3Me_2$); 118.5, 118.2 (CH); 95.7 (C^2CCH); 89.3, 88.1 (Cp); 81.2 (C^2); 46.5 (NMe); 45.7 ($C^3\mathit{Me}$); 20.0, 19.3 ($C_6H_3\mathit{Me}_2$). ESI-MS (ES^+): 547 m/z [M^+].

Reaction of [2b]SO_3CF_3 with Ph_3PCH_2/NaH/CF_3SO_3H: formation of [$Fe_2Cp_2(CO)(\mu\text{-}CO)\{\mu\text{-}\eta^1\text{:}\eta^2\text{-}C^3(Me)C^2(CH_2)C^1N(Me)(Xyl)\}$], 4, and [2c]$SO_3CF_3$ (Chart 4).[12]

Chart 4. Structures of E-**4** and Z-[**2c**]$^+$.

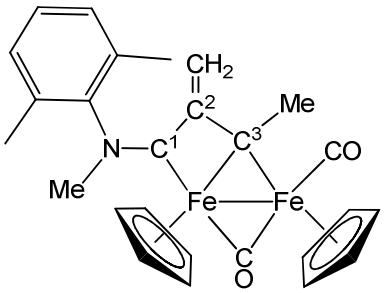

E-**4**

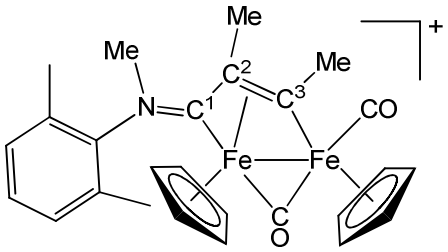

Z-[**2c**]$^+$

The reaction of [**2b**]SO_3CF_3 (152 mg, 0.240 mmol) with Ph_3PCH_2 (265 mg, 0.959 mmol) and NaH (17 mg, 0.71 mmol) was carried out by a procedure similar to that described for the synthesis of **3**. After 30 minutes, the IR spectrum of the mixture cleanly exhibited two bands (1952vs, 1773s), assigned to **4**. Every attempts of purification through stationary phases resulted in prevalent decomposition. Thus the liquid phase was separated and treated with CF_3SO_3H (0.022 mL, 0.249 mmol). Clean formation of cis-[**2c**]SO_3CF_3 was recognized after 5 minutes by IR spectroscopy. The product was purified by alumina chromatography and finally obtained as a dark-red solid. Yield: 117 mg, 75%. Anal. Calcd. for $C_{27}H_{28}F_3Fe_2NO_5S$: C, 50.10; H, 4.36; N, 2.16. Found: C, 49.86; H, 4.28; N, 2.18. IR (CH_2Cl_2): ν/cm^{-1} = 1987vs (CO), 1819s (μ-CO), 1610m (NC^1C^2). ^1H NMR ($CDCl_3$): δ/ppm = 7.48-7.00 (3 H, $C_6H_3Me_2$); 5.29, 4.68 (s, 10 H, Cp); 3.88, (s, 3 H, C^3Me); 3.37 (s, 3 H, NMe); 2.49, 1.99 (s, 6 H, $C_6H_3Me_2$); 2.10 (s, 3 H, C^2Me).

Synthesis of [$Fe_2Cp_2(CO)(\mu\text{-}CO)\{\mu\text{-}\eta^1\text{:}\eta^3\text{-}C^3(Me)C^2(CH_2Ph)C^1N(Me)(Xyl)\}$]Br, [5]Br, and isomerization reaction (Chart 5).

Chart 5. Structures of E-[**5**]$^+$ and Z-[**5**]$^+$.

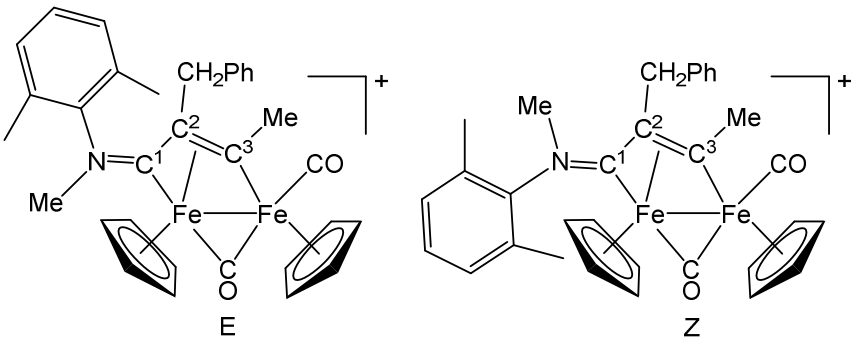

The synthesis of [**5**]Br was carried out by a procedure analogous to that described for the synthesis of **3** (reaction time = 24 hours). The final mixture was dried under reduced pressure, then the residue was dissolved in dichloromethane and quickly chromatographed through a short alumina pad. After washing with THF, a fraction was collected using neat MeOH as eluent. The title compound was isolated as isomeric mixture (E-Z) upon removal of the solvent under reduced pressure. Full conversion into the Z isomer was achieved by heating a solution of the mixture in MeOH for 40 minutes at ca. 50 °C. The final product was purified by filtration on a short alumina column, and then obtained as a crystalline solid upon slow evaporation of the solvent from the methanol solution.

E-[5]Br + **Z-[5]Br**. Brown solid, from [**2b**]SO_3CF_3 (180 mg, 0.284 mmol), $PhCH_2Br$ (0.31 mL, 2.6 mmol) and NaH (21 mg, 0.88 mmol). Yield 113 mg, 55%. Anal. Calcd. for $C_{32}H_{32}BrFe_2NO_2$: C, 58.75; H, 4.93; N, 2.14; Br, 12.21. Found: C, 58.38; H, 4.98; N, 2.26; Br, 11.89. IR (CH_2Cl_2): ν/cm^{-1} = 1986vs (CO), 1814s (μ-CO), 1603m (NC^1C^2), 1586w (C=C). ^{1}H NMR ($CDCl_3$): δ/ppm = 7.42-7.05 (8 H, Ph + $C_6H_3Me_2$); *5.49*, 5.44, 5.24, *4.99* (s, 10 H, Cp); 4.57, 4.47 (d, 2 H, $^2J_{HH}$ = 19.9 Hz, CH_2); 4.10, *3.15* (s, 3 H, NMe); *3.99*, 3.87 (s, 3 H, C^3Me); *2.57*, 2.32, *2.01*, 1.74 (s, 6 H, $C_6H_3Me_2$). E/Z ratio = 2. $^{13}C\{^1H\}$ NMR ($CDCl_3$): δ/ppm = 254.7, *254.4* (μ-CO); 233.2, *232.5* (C^1); 211.5, *211.3*, *210.5*, 209.6 (CO + C^3); 144.6, *140.6* (*ipso*-$C_6H_3Me_2$); 131.5-126.9 (Ph + $C_6H_3Me_2$); 90.9, *90.6*, 87.7, *87.4* (Cp); 64.4, *63.8* (C^2); 59.0 (CH_2); *52.1*, 46.1 (NMe); 43.0, *42.5* (C^3Me); 18.2, *18.1*, *17.5*, 17.0 ($C_6H_3Me_2$).

Z-[5]Br. Light brown solid, yield 70%. Anal. Calcd. for $C_{32}H_{32}BrFe_2NO_2$: C, 58.75; H, 4.93; N, 2.14; Br, 12.21. Found: C, 58.41; H, 5.03; N, 2.20; Br, 12.04. IR (CH_2Cl_2): ν/cm^{-1} = 1981vs (CO), 1818s (μ-CO), 1613m (NC^1C^2), 1587w (C=C). ^{1}H NMR ($CDCl_3$): δ/ppm = 7.43-7.34 (8 H, Ph + $C_6H_3Me_2$); 5.49, 4.99 (s, 10 H, Cp); 4.62, 4.58 (m, 2 H, CH_2); 3.99 (s, 3 H, C^3Me); 3.15 (s, 3 H, NMe); 2.57, 2.01 (s, 6 H, $C_6H_3Me_2$). $^{13}C\{^1H\}$ NMR (dmso-d_6): δ/ppm = 254.8 (μ-CO); 229.5 (C^1); 212.6 (CO); 206.8 (C^3); 162.6 (*ipso*-Ph); 141.1 (*ipso*-$C_6H_3Me_2$); 138.3, 134.3, 130.0, 129.8, 129.4, 128.0, 127.2 (Ph + $C_6H_3Me_2$); 92.4, 88.8 (Cp); 66.6 (C^2); 58.4 (CH_2); 50.9 (NMe); 38.2 (C^3Me); 18.2 ($C_6H_3Me_2$).

Reaction of [2c]SO_3CF_3 with PhSSPh/NaH: synthesis of [Fe_2Cp_2(SPh)(CO)(μ-CO){μ-C^1N(Me)(Xyl)}], 6 (Chart 6).

Chart 6. Structure of **6**.

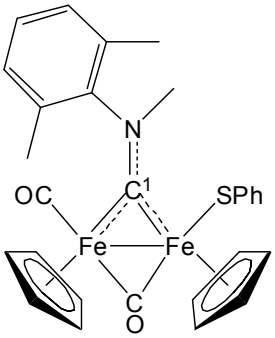

To a stirred solution of cis-[**2c**]SO_3CF_3 (120 mg, 0.185 mmol), in tetrahydrofuran (15 mL), PhSSPh (295 mg, 1.35 mmol) and then NaH (23 mg, 0.96 mmol) were added. The resulting mixture was stirred overnight. Hence, the volatile materials were removed under vacuum. The residue was dissolved in CH_2Cl_2 and filtered through alumina. Compound **6** was recovered as a red microcrystalline powder upon removal of the solvent. Yield 70 mg, 68%. Anal. Calcd. for $C_{28}H_{27}Fe_2NO_2S$: C, 60.78; H, 4.92; N, 2.53. Found: C, 60.63; H, 5.01; N, 2.49. IR (CH_2Cl_2): ν/cm^{-1} = 1969vs (CO), 1791s (μ-CO), 1512m (C^1N). ^{1}H NMR ($CDCl_3$): δ/ppm = 7.49-7.00 (5 H, Ph + $C_6H_3Me_2$); 4.68, 4.26 (s, 10 H, Cp); 4.64 (s, 3 H, NMe); 2.71, 2.25 (s, 6 H, $C_6H_3Me_2$). $^{13}C\{^1H\}$ NMR ($CDCl_3$): δ/ppm = 338.5 (C^1); 265.0 (μ-CO);

213.8 (CO); 148.5 (*ipso*-$C_6H_3Me_2$); 137.0-123.2 (Ph + $C_6H_3Me_2$); 87.5, 86.1 (Cp); 51.2 (NMe); 18.5, 17.7 ($C_6H_3Me_2$).

Reaction of [2d]SO_3CF_3 with PhSSPh/NaH: synthesis of [$Fe_2Cp_2(CO)(\mu\text{-}CO)\{\mu\text{-}\eta^1\text{:}\eta^2\text{-}C^3(Me)C^2(Me)(SPh)C^1N(Me)_2\}$], 7 (Chart 7).

Chart 7. Structure of **7**.

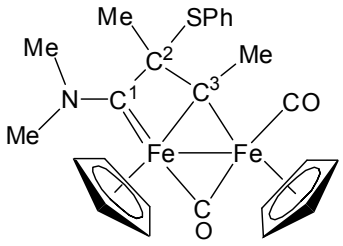

To a stirred solution of [**2d**]SO_3CF_3 (130 mg, 0.233 mmol), in THF (15 mL), PhSSPh (320 mg, 1.47 mmol) and then NaH (23 mg, 0.96 mmol) were added. The resulting mixture was stirred for 1 h, then it was filtered on a short alumina pad. Addition of diethyl ether (50 mL) gave a green precipitate which was isolated and dried under vacuum. Yield 66 mg, 55%. Anal. Calcd. for $C_{25}H_{27}Fe_2NO_2S$: C, 58.05; H, 5.26; N, 2.71. Found: C, 58.13; H, 5.39; N, 2.66. IR (CH_2Cl_2): ν/cm^{-1} = 1929vs (CO), 1752s (μ-CO), 1624w (C^1N). ^1H NMR ($CDCl_3$): δ/ppm = 7.58-6.84 (5 H, Ph); 4.61, 4.39 (s, 10 H, Cp); 3.71 (s, 3 H, C^3Me); 3.51, 3.00 (s, 6 H, NMe_2); 1.37 (s, 3 H, C^2Me). $^{13}C\{^1H\}$ NMR ($CDCl_3$): δ/ppm = 278.4 (μ-CO); 251.6 (C^1); 215.7 (CO); 177.0 (C^3); 152.6 (*ipso*-Ph); 144.7-122.8 (Ph); 87.2, 86.5 (Cp); 84.3 (C^2); 46.3, 45.8 (NMe_2); 43.6 (C^3*Me*); 29.5 (C^2*Me*).

Computational studies. All the geometries were optimized with ORCA 4.0.1.2,[39] using the B97 functional[40] in conjunction with a triple-ζ quality basis set (def2-TZVP). The dispersion corrections were taken into account using the Grimme D3-parametrized correction and the with Becke-Jonhson damping to the DFT energy.[41] All the structures were confirmed to be local energy minima (no

imaginary frequencies) for intermediate species and saddle points (one imaginary frequency) for transition states. In some cases, an unavoidable very low negative frequency is present, correlated to the rotation of the Cp moiety around the Cp-Fe bond axis.

X-ray crystallography

Crystal data and collection details for [**2a**]SO_3CF_3 are reported in Table S3. Data were recorded on a Bruker APEX II diffractometer equipped with a PHOTON100 detector using Mo–Kα radiation. Data were corrected for Lorentz polarization and absorption effects (empirical absorption correction SADABS).[42] The structure was solved by direct methods and refined by full-matrix least-squares based on all data using F^2.[43]

Supporting Information.

DFT optimized geometries of compounds; IR and NMR spectra. The file "DFTgeometries.xyz" contains the computed Cartesian coordinates of all of the compounds reported in this study. The file can be opened as a text file to read the coordinates, or with a molecular modeling program such as Mercury (version 3.3 or later, http://www.ccdc.cam.ac.uk/pages/Home.aspx) for visualization and analysis. CCDC reference number 1849098 ([**2a**]SO_3CF_3) contains the supplementary crystallographic data for the X-ray study reported in this paper. These data can be obtained free of charge at www.ccdc.cam.ac.uk/conts/retrieving.html (or from the Cambridge Crystallographic Data Centre, 12, Union Road, Cambridge CB2 1EZ, UK; fax: (internat.) +44-1223/336-033; e-mail: deposit@ccdc.cam.ac.uk).

Corresponding Authors

*E-mail addresses: gianluca.ciancaleoni@unipi.it; fabio.marchetti1974@unipi.it

Notes

The authors declare no competing financial interest.

Acknowledgement

We thank the *Universities of Bologna and Pisa* for financial support.

References

1 Selected recent references: (a) Rocchigiani, L.; Fernandez-Cestau, J.; Agonigi, G.; Chambrier, I.; Budzelaar, P. H. M.; Bochmann, M., Gold(III) Alkyne Complexes: Bonding and Reaction Pathways, *Angew. Chem., Int. Ed*. **2017**, *56*, 13861-13865. (b) Kaneko, T.; Murotani, E.; Tenjimbayashi, R.; Suzuki, H.; Takao, T., Photolysis of triruthenium μ3-alkyne complexes capped by a μ3-oxo ligand, *J. Organomet. Chem.* **2016**, *812*, 167-176. (c) Baldridge, K. K.; Bunker, K. D.; Velez, C. L.; Holland, R. L.; Rheingold, A. L.; Moore, C. E.; O'Connor, J. M., Structural Characterization of (C5H5)Co(PPh3)(η2-alkyne) and (C5H5)Co(η2-alkyne) Complexes of Highly Polarized Alkynes, *Organometallics* **2013**, *32*, 5473-5480. (d) Adams, H.; Booth, Y. K.; Cook, E. S.; Riley, S.; Morris, M. J. Reactions of Tetracyclone Molybdenum Complexes with Electrophilic Alkynes: Cyclopentadienone-Alkyne Coupling and Alkyne Coordination, *Organometallics* **2017**, *36*, 2254-2261. (e) Parker, K. D. J.; Fryzuk, M. D., Synthesis, Structure, and Reactivity of Niobium and Tantalum Alkyne Complexes, *Organometallics* **2015**, *34*, 2037-2047.

2 Selected references: (a) Zeni, G.; Larock, R. C. Synthesis of Heterocycles via Palladium π-Olefin and π-Alkyne Chemistry, *Chem. Rev.* **2004**, *104*, 2285-2309. (b) Salvio, R.; Julia-Hernandez, F.; Pisciottani, L.; Mendoza-Merono, R.; Garcia-Granda, S.; Bassetti, M. Kinetics and Mechanistic Insights into the Acetate-Assisted Dimerization of Terminal Alkynes under Ruthenium- and Acid-Promoted (RAP) Catalysis, *Organometallics* **2017**, *36*, 3830-3840. (c) Mandal, R.; Sundararaju, B., Cp*Co(III)-Catalyzed Annulation of Carboxylic Acids with Alkynes, *Org. Lett.* **2017**, *19*, 2544-2547. (d) Azpiroz, R.; Rubio-Perez, L.; Di Giuseppe, A.; Passarelli, V.; Lahoz, F. J.; Castarlenas, R.; Perez-Torrente, J. J.; Oro, L. A., Rhodium(I)-N-Heterocyclic Carbene Catalyst for Selective Coupling of N-Vinylpyrazoles with Alkynes via C-H Activation, *ACS Catal*., **2014**, *4*, 4244-4253. (e) Zeng, M.; Li, Le; H., Seth B., A Highly Active and Air-Stable Ruthenium Complex for the Ambient Temperature Anti-Markovnikov Reductive Hydration of Terminal Alkynes, *J. Am. Chem. Soc*., **2014**, *136*, 7058-7067. (f) MacDougall, T. J.; Llamazares, A.; Kuhnert, O.; Ferguson, M. J.; McDonald, R.; Cowie, M. Alkyne/methylene coupling at adjacent iridium/osmium centers: facile carbon-carbon and carbon-oxygen bond formation *Organometallics* **2011**,

30, 952-964. (g) Knorr, M.; Jourdain, I. Activation of alkynes by diphosphine- and μ-phosphido-spanned heterobimetallic complexes, *Coord. Chem. Rev*. **2017**, *350*, 217-247.

3 See for instance: (a) García, M. E.; García-Vivó, D.; Menéndez, S.; Ruiz, M. A. C–C and C–N Couplings in Reactions of the Benzylidyne-Bridged Complex [Mo2Cp2(μ-CPh)(μ-PCy2)(CO)2] with Small Unsaturated Organics, *Organometallics* **2016**, *35*, 3498−3506. (b) Alvarez, M. A.; García, M. E.; González, R.; Ruiz, M. A. Reactions of the Phosphinidene-Bridged Complexes [Fe2(η5-C5H5)2(μ-PR)(μ-CO)(CO)2] (R = Cy, Ph, 2,4,6-C6H2tBu3) with Diazoalkanes. Formation and Rearrangements of Phosphadiazadiene-Bridged Derivatives, *Organometallics* **2013**, *32*, 4601 − 4611. (c) Dennett, J. N. L.; Knox, S. A. R.; Anderson, K. M.; Charmant, J. P. H.; Guy Orpen, A. The synthesis of [FeRu(CO)2(CO)2(C5H5)(C5Me5)] and convenient entries to its organometallic chemistry, *Dalton Trans.* **2005**, 63–73. (d) Wigginton, J. R.; Chokshi, A.; Graham, T. W.; McDonald, R.; Ferguson, M. J.; Cowie, M. Alkyne/Methylene Coupling Reactions at Adjacent Rh/Os Centers: Stepwise Transformations from C1- through C4-Bridged Species *Organometallics* **2005**, *24*, 6398-6410. (e) Knorr, M.; Jourdain, I.; Braunstein, P.; Strohmann, C.; Tiripicchio, A.; Ugozzoli, F., Insertion reactions of alkynes and organic isocyanides into the palladium-carbon bond of dimetallic Fe-Pd alkoxysilyl complexes, *Dalton Trans.* **2006**, *44*, 5248-5258. (f) Rowsell, B. D.; McDonald, R.; Ferguson, M. J.; Cowie, M. Carbon-Carbon Bond Formation Promoted by Adjacent Metal Centers: Regioselective Alkyne Insertions into a "Rh(μ-CH2)Ru" Moiety Yielding C3- and C5-Bridged Fragments *Organometallics* **2003**, *22*, 2944-2955.

4 a) Labinger, J. A. Does cyclopentadienyl iron dicarbonyl dimer have a metal–metal bond? Who's asking?, *Inorg. Chim. Acta* **2015**, *424*, 14–19. b) Bitterwolf, T. E. Photochemistry and reaction intermediates of the bimetallic Group VIII cyclopentadienyl metal carbonyl compounds, (η5-C5H5)2M2(CO)4 and their derivatives, *Coord. Chem. Rev*. **2000**, *206-207*, 419-450.

5 Selected references: (a) Mazzoni, R.; Salmi, M.; Zanotti, V. C-C Bond Formation in Diiron Complexes, *Chem. Eur. J*. **2012**, *18*, 10174-10194. (b) Liu, Y.; Wang, R.; Sun, J.; Chen, J. Reactions of Cationic Bridging Carbyne Complexes of Bis(η-cyclopentadienyl)diiron Tricarbonyl with Nucleophiles. A Route to Diiron Bridging Carbene Complexes, *Organometallics* **2000**, *19*, 3498-3506. (c) Etienne, M.; Talarin, J.; Toupet, L. Syntheses and physicochemical properties of polycyano-substituted buta-1,3-dienylidene- and allenylidene-bridged diiron complexes, *Organometallics* **1992**, *11*, 2058-2068. (d) Casey, C. P.; Crocker, M.; Vosejpka, P. C. Reactions of organocopper reagents with the cationic bridging acylium complex [C5H5(CO)Fe]2(.mu.-CO)(.mu.-CHCO)+, *Organometallics* **1989**, *8*, 278-282. (e) Casey, C. P.; Crocker, M.; Niccolai, G. P.; Fagan, P. J.; Konings, M. S. Formation of bridging acylium and nitrilium complexes by reaction of carbon monoxide and tert-butyl isocyanide with a bridging diiron methylidyne complex. Evidence for strong electron donation from the Fe2C core onto the .mu.-CHC.tplbond.O and .mu.-CHC.tplbond.NR ligands, *J. Am. Chem. Soc*. **1988**, *110*, 6070-6076. (f) Heel, E. L.; Ansell, G. B.; Leta, S.

Synthesis and characterization of (.mu.-cyclopropylidene)diiron complexes [cyclic] cis- and trans-(.eta.5-C5H5)2Fe2(CO)2(.mu.-CO)(.mu.-CCH2CH2). Models for intermediates in hydrocarbation and Fischer-Tropsch mechanisms, *Organometallics* **1984**, *3*, 1633-1637.

6 *Selected references*: (a) He, J.; Deng, C.-L.; Li, Y.; Li, Y.-L.; Wu, Y.; Zou, L.-K.; Mu, C.; Luo, Q.; Xie, B.; Wei, J. A New Route to the Synthesis of Phosphine-Substituted Diiron Aza- and Oxadithiolate Complexes, *Organometallics* **2017**, *36*, 1322-1330. (b) Tong, P.; Yang, D.; Li, Y.; Wang, B.; Qu, J. Hydration of Nitriles to Amides by Thiolate-Bridged Diiron Complexes *Organometallics* **2015**, *34*, 3571−3576. c) Chen, Y.; Liu, L.; Peng, Y.; Chen, P.; Luo, Y.; Qu, J. Unusual Thiolate-Bridged Diiron Clusters Bearing the cis-HN═NH Ligand and Their Reactivities with Terminal Alkynes *J. Am. Chem. Soc.* **2011**, *133*, 1147-1149. (d) Alvarez, M. A.; García, M. E.; González, R.; Ruiz, M. A. Reactions of the phosphinidene-bridged complexes [Fe2(η5-C5H5)2(μ-PR)(μ-CO)(CO)2] (R = Cy, Ph) with electrophiles based on p-block elements *Dalton Trans*. **2012**, *41*, 14498-14513. (e) Alvarez, M. A.; García, M. E.; González, R.; Ruiz, M. A. Reactions of the Phosphinidene-Bridged Complexes [Fe2(η5-C5H5)2(μ-PR)(μ-CO)(CO)2] (R = Cy, Ph, 2,4,6-C6H2tBu3) with Diazoalkanes. Formation and Rearrangements of Phosphadiazadiene-Bridged Derivatives, *Organometallics* **2010**, 29, 5140–5153. (f) Marchetti, F. Constructing Organometallic Architectures from Aminoalkylidyne Diiron Complexes, DOI 10.1002/ejic.201800659.

7 (a) Bauer, I.; Knolker, H. J. Iron Catalysis in Organic Synthesis, *Chem. Rev*. **2015**, *115*, 3170-3387. (b) Fürstner, A. *ACS Cent. Sci*. **2016**, *2*, 778. (c) Fukuzumi, S.; Lee, Y.-M.; Nam, W. Thermal and photocatalytic production of hydrogen with earth-abundant metal complexes, *Coord. Chem. Rev*. **2018**, *355*, 54–73. (d) Takeda, H.; Cometto, C.; Ishitani, O.; Robert, M. Electrons, Photons, Protons and Earth-Abundant Metal Complexes for Molecular Catalysis of CO2 Reduction, *ACS Catal*. **2017**, *7*, 70−88. (e) Hunter, B. M.; Gray, H. B.; Müller, A. M. Earth-Abundant Heterogeneous Water Oxidation Catalysts, *Chem. Rev*. **2016**, *116*, 14120-14136. (f) Su, B.; Cao, Z.-C.; Shi, Z.-J. Exploration of Earth-Abundant Transition Metals (Fe, Co, and Ni) as Catalysts in Unreactive Chemical Bond Activations, *Acc. Chem. Res*. **2015**, *48*, 886−896.

8 (a) Kurtz, D. M.; Boice, E.; Caranto, J. D.; Frederick, R. E.; Masitas, C. A.; Miner, K. D. *Encyclopedia of Inorganic and Bioinorganic Chemistry* **2013**, 1-18. (b) Wang, V. C.-C.; Maji, S.; Chen, P.-Y.; Lee, H. K.; Yu, S.-F.; Chan, S.-F. Alkane Oxidation: Methane Monooxygenases, Related Enzymes, and Their Biomimetics, C*hem. Rev*. **2017**, *117*, 8574-8621. (c) Senger, M.; Laun, K.; Wittkamp, F.; Duan, J.; Haumann, M.; Happe, T.; Winkler, M.; Apfel, U.-P.; Stripp, S. T. Proton-Coupled Reduction of the Catalytic [4Fe-4S] Cluster in [FeFe]-Hydrogenases, *Angew. Chem., Int. Ed*. **2017**, *56*, 16503-16506. (d) May, B.; Young, L.; Moore, A. L. Structural insights into the alternative oxidases: are all oxidases made equal?, *Biochem. Soc. Trans*. **2017**, *45*, 731-740.

9 (a) Dyke, A. F.; Knox, S. A. R.; Naish, P. J.; Taylor, G. E. Organic chemistry of dinuclear metal centres. Part 1. Combination of alkynes with carbon monoxide at di-iron and diruthenium centres: crystal structure of $[Ru_2(CO)(\mu\text{-}CO)\{\mu\text{-}\sigma\text{:}\eta^3\text{-}C(O)C2Ph_2\}(\eta\text{-}C_5H_5)_2]$, J. Chem. Soc. Dalton Trans. 1982, 1297-1307. (b) Boni, A.; Funaioli, T.; Marchetti, F.; Pampaloni, G.; Pinzino, C.; Zacchini, S. Electrochemical, EPR and computational results on $[Fe_2Cp_2(CO)_2]$-based complexes with a bridging hydrocarbyl ligand, *J. Organomet. Chem*. **2011**, *696*, 3551-3556.

10 Marchetti, F.; Zacchini S.; Zanotti, V. Photochemical Alkyne Insertions into the Iron–Thiocarbonyl Bond of $[Fe_2(CS)(CO)_3(Cp)_2]$, *Organometallics* **2016**, *35*, 2630−2637.

11 Albano, V. G.; Busetto, L.; Marchetti, F.; Monari, M.; Zacchini, S.; Zanotti, V. Alkyne Isocyanide Coupling in [Fe2(CNMe)(CO)3(Cp)2]: a new route to diiron μ-vinyliminium complexes, *Organometallics* **2007**, *26*, 3448-3455.

12 (a) Albano, V. G.; Busetto, L.; Marchetti, F.; Monari, M.; Zacchini, S.; Zanotti, V. Diiron μ-Vinyliminium Complexes from Acetylene Insertion into a Metal−Aminocarbyne Bond, *Organometallics*, **2003**, *22*, 1326-1331. (b) Albano, V. G.; Busetto, L.; Marchetti, F.; Monari, M.; Zacchini, S.; Zanotti, V. Stereochemistry of the insertion of disubstituted alkynes into the metal aminocarbyne bond in diiron complexes, *J. Organomet. Chem.*, **2004**, *689*, 528–538.

13 (a) Churchill, M. R.; Lake, C. H.; Lashewycz-Rubycz, R. A.; Yao, H.; McCargar, R. D.; Keister, J. B. Structural studies on ruthenium carbonyl hydrides: XVIII. Synthesis and characterization of (μ-H)Ru3(μ3-η3-XCCRCR′)(CO)9-n(PPh3)n complexes. Crystal structures of (μ-H)Ru3(μ3-η3-Et2NCCHCMe)(CO)8(PPh3) and (μ-H)Ru3(μ3-η3-MeOCCMeCMe)(CO)7(PPh3)2·2CH2Cl2 *J. Organomet. Chem.* **1993**, *452*, 151-160. (b) Aime, S.; Osella, D.; Deeming, A. J.; Arce, A. J.; Hursthouse, M. B.; Dawes, H. M. Molecular structures and dynamic behaviour of two isomers of [Ru3(μ-H)(μ3-Me2NC4H4)(CO)9] formed from 1-dimethylaminobut-2-yne and containing η2-alkene-1,3-diyl and η2-alkene-1,2-diyl ligands respectively *J. Chem. Soc., Dalton Trans*. **1986**, 1459-1463. (c) Aime, S.; Osella, D.; Arce, A. J.; Deeming, A. J.; Hursthouse, M. B.; Galas, A. M. R. Synthesis, structure, and isomerisation of triruthenium and triosmium clusters derived from 3-dimethylaminoprop-1-yne; *X*-ray crystal structure of [Ru3–H(CO)9(Me2N═C–C═CH2)] *J. Chem. Soc., Dalton Trans*. **1984**, 1981-1986.

14 See for instance: (a) Chiang, K. P.; Bellows, S. M.; Brennessel, W. W.; Holland, P. L. Multimetallic cooperativity in activation of dinitrogen at iron–potassium sites, *Chem. Sci*. **2014**, *5*, 267-274. (b) McInnis, J. P.; Delferro, M.; Marks, T. J. Multinuclear Group 4 Catalysis: Olefin Polymerization Pathways Modified by Strong Metal–Metal Cooperative Effects *Acc. Chem. Res*. **2014**, *47*, 2545-2557. (c) Huang, G.-H.; Li, J.-M.; Huang, J.-J.; Lin, J.-D.; Chuang, G. J. Cooperative Effect of Two Metals: CoPd(OAc)4-Catalyzed C□H Amination and Aziridination *Chem. Eur. J.* **2014**, *20*, 5240-5243. (d) Patureau, F. W.; de Boer, S.; Kuil, M.; Meeuwissen, J.; Breuil, P.-A. R.; Siegler, M. A.; Spek, A. L.; Sandee, A. J.; de Bruin, B.; Reek, J.

N. H. Sulfonamido−Phosphoramidite Ligands in Cooperative Dinuclear Hydrogenation Catalysis *J. Am. Chem. Soc.* **2009**, *131*, 6683-6685. (e) Saouma, C. T.; Müller, P.; Peters, J. C. Characterization of Structurally Unusual Diiron NxHy Complexes *J. Am. Chem. Soc*. **2009**, *131*, 10358–10359. (f) Torkelson, J. R.; Antwi-Nsiah, F. H.; McDonald, R.; Cowie, M.; Pruis, J. G.; Jalkanen, K. J.; DeKock, R. L. Metal-Metal Cooperativity Effects in Promoting C-H Bond Cleavage of a Methyl Group by an Adjacent Metal Center *J. Am. Chem. Soc*. **1999**, *121*, 3666-3683.

15 (a) Marchetti, F.; Zacchini, S.; Zanotti, V. Amination of Bridging Vinyliminium Ligands in Diiron Complexes: C-N Bond Forming Reactions for Amidine-Alkylidene Species, *Organometallics* **2018**, *37*, 107-115, and references therein. b) Albano, V. G.; Busetto, L.; Marchetti, F.; Monari, M.; Zacchini, S.; Zanotti, V. Regio- and Stereoselective Hydride Addition at μ-Vinyliminium Ligands in Cationic Diiron Complexes, *Organometallics* **2004**, *23*, 3348-3354.

16 See for instance (and references therein): (a) Marchetti, F.; Zacchini, S.; Salmi, M.; Busetto, L.; Zanotti, V. C–H Activation in Diiron Bridging Vinyliminium Ligands: Reaction with CS2 to Form New Zwitterionic Complexes Acting as Organometallic Ligands, *Eur. J. Inorg. Chem.* **2011**, 1260–1268. (b) Busetto, L.; Marchetti, F.; Renili, F.; Zacchini, S.; Zanotti, V. Addition of Alkynes to Zwitterionic μ-Vinyliminium Diiron Complexes: New Selenophene (Thiophene) and Vinyl Chalcogenide Functionalized Bridging Ligands, *Organometallics* **2010**, *29*, 1797–1805

17 (a) Busetto, L.; Marchetti, F.; Mazzoni, R.; Salmi, M.; Zacchini, S.; Zanotti, V. [3+2+1] cycloaddition involving alkynes, CO and bridging vinyliminium ligands in diiron complexes: a dinuclear version of the Dötz reaction?, *Chem. Commun*., **2010**, *46*, 3327–3329. (b) Busetto, L.; Mazzoni, R.; Salmi, M.; Zacchini, S.; Zanotti, V. Ferrocenes Containing a Pendant Propargylic Chain Obtained via Addition of Propargyl Alcohol to μ-Vinyliminium Ligands in Diiron Complexes, *Organometallics* **2012**, *31*, 2667-2674.

18 Marchetti, F.; Zacchini, S.; Zanotti, V. C–S and C–Se Bond Formation at Bridging Vinyliminium Ligands in Diiron Complexes, *Eur. J. Inorg. Chem*. **2013**, 5145–5152.

19 Bursten, B. E.; McKee, S. D.; Platz, M. S. Photochemical insertion of alkynes into iron complex Cp2Fe2(CO)2(μ–CO)2: a mechanistic study by laser flash photolysis, *J. Am. Chem. Soc*. **1989**, *111*, 3428-3429.

20 Agonigi, G.; Bortoluzzi, M.; Marchetti, F.; Pampaloni, G.; Zacchini, S.; Zanotti, V. Regioselective Nucleophilic Additions to Diiron Carbonyl Complexes Containing a Bridging Aminocarbyne Ligand: A Synthetic, Crystallographic and DFT Study, *Eur. J. Inorg. Chem.* **2018**, 960–971.

21 S. Willis, A. R. Manning, F. S. Stephens, Reactions of [Fe2(dienyl)n(CO)(CNR)] Complexes (dienyl = C5H8, C5H4Me8 or C9H7; R = alkyl or benzyl) with Alkyl Halides and Other Alkylating Agents. The Crystal Structure of cis-[Fe2(C5H4Me)2(CO)3(CNMe2)]+, *J. Chem. Soc., Dalton Trans*., **1980**, 186-191.

22 Bridgeman, A. J.; Cavigliasso, G.; Ireland, L. R.; Rothery, J. The Mayer bond order as a tool in inorganic chemistry, J. Chem. Soc., *Dalton Trans*., **2001**, 2095–2108.

23 Farrugia, L. J. Dynamics and fluxionality in metal carbonyl clusters: some old and new problems, J. Chem. Soc., *Dalton Trans*. **1997**, 1783–1792.

24 Albano, V. G.; Busetto, L.; Marchetti, F.; Monari, M.; Zacchini, S.; Zanotti, V. C–C bond formation by cyanide addition to dinuclear vinyliminium complexes, *J. Organomet. Chem.* **2006**, *691*, 4234–4243.

25 (a) Busetto, L.; Marchetti, F.; Zacchini, S.; Zanotti, V. Acetylide Addition to Bridging Vinyliminium Ligands in Dinuclear Complexes, *Eur. J. Inorg. Chem.* **2007**, 1799–1807. (b) Busetto, L.; Marchetti, F.; Zacchini, S.; Zanotti, V. CO Cleavage Promoted by Acetylide Addition to Vinyliminium Diiron Complexes. *Eur. J. Inorg. Chem.* **2006**, 285–289.

26 Busetto, L.; Marchetti, F.; Zacchini, S.; Zanotti, V. Addition of Isocyanides at Diiron μ-Vinyliminium Complexes: Synthesis of Novel Ketenimine−Bis(alkylidene) Complexes, *Organometallics* **2008**, *27*, 5058–5066.

27 Coşkun, N.; Erden, I. An efficient catalytic method for fulvene synthesis, *Tetrahedron*, **2011**, *67*, 8607-8614.

28 Busetto, L.; Marchetti, F.; Zacchini, S.; Zanotti, V. Unprecedented Zwitterionic Iminium - Chalcogenide Bridging Ligands in Diiron Complexes, *Organometallics* **2006**, *25*, 4808-4816, and references therein.

29 $[Fe_2Cp_2(CO)(\mu\text{-}CO)\{\mu\text{-}\eta^1\text{:}\eta^2\text{-}C(Me)C(O)CN(Me)(Xyl)\}]$ [28]. IR (CH_2Cl_2): ν/cm^{-1} = 1945vs (CO), 1777s (μ-CO), 1550m ($C^1N + C^2{=}C^3$). $^{13}C\{^1H\}$ NMR ($CDCl_3$): δ/ppm = 258.9 (C^1); 184.5 (C3).

30 (a) Edwards, A. J.; Koehler, J. U.; Lewis, J.; Raithby, P. R., Reaction of a side-on coordinated carbene ligand with the Wittig reagent, *J. Chem. Soc., Dalton Trans*. **1995**, *19*, 3251-3252. (b) Casey, C. P.; Burkhardt, T. J. Reaction of metal-carbene complexes with Wittig reagents. New vinyl ether synthesis , *J. Am. Chem. Soc*. **1972**, *94*, 6543-6544.

31 (a) Tashtoush, H. I.; Sustmann, R. Chromium(II)-mediated intermolecular free-radical carbon-carbon bond formation, *Chem. Ber.* **1992**, *125*, 287-289. (b) Hwang, W. S.; Liao, R. Li; Horng, Y. L.; Ong, C. W. Electrochemical reactions of tricarbonyl(cyclohexadienylium)iron salt: regiochemistry during the cross coupling reaction and trapping of the 19-electron transient tricarbonyl(cyclohexadienyl radical)iron species, *Polyhedron* **1989**, *8*, 479-482.

32 Connelly, N. G.; Geiger, W. E. Chemical Redox Agents for Organometallic Chemistry, *Chem. Rev*. **1996**, *96*, 877−910.

33 Marchetti, F.; Zacchini, S.; Zanotti, V. Unprecedented Transformation of Diiron Bridging Vinyliminium Ligands into Carboxyamido and Alkylphosphonate-Vinylalkylidenes, *Eur. J. Inorg. Chem*. **2012**, 2456–2463.

34 (a) Alvarez, A. M.; García, M. E.; García-Vivó, D.; Ruiz, M. A.; Vega, M. F., Insertion, Rearrangement, and Coupling Processes in the Reactions of the Unsaturated Hydride Complex [W2(η5-C5H5) 2(H)(μ-PCy2)(CO)2] with Isocyanides, *Organometallics* **2013**, *32*, 4543-4555. (b) Zhou, X.; Barton, B. E.; Chambers, G. M.; Rauchfuss, T. B. Preparation and Protonation of Fe2(pdt)(CNR)6, Electron-Rich Analogues of Fe2(pdt)(CO)6, *Inorg. Chem*. **2016**, *55*, 3401−3412. (c) Cabon, N.; Paugam, E.; Pétillon, F. Y.; Schollhammer, P.; Talarmin, J., Unexpected Coupling of Cp and Two RNC Ligands at a {Mo2(SMe)3} Nucleus, *Organometallics* **2003**, *22*, 4178 – 4180. (d) Knorr, M.; Strohmann, C. Synthesis, Reactivity, and Molecular Structures of Bis(diphenylphosphanyl)-amine- and Bis(diphenylphosphanyl)amide-Bridged Heterobimetallic Isonitrile- and Aminocarbyne Complexes (Fe-Pt), *Eur. J. Inorg. Chem*. **1998**, 495-499. (e) Boss, K.; Dowling, C.; Manning, A. R. Preparation, spectra and structure of [Fe2(C5H5)2(L)(CN)(CO){CN(R')R}], [Fe2(C5H5)2(CO)(CN){CNMe2}2]$^{+}$ and [Fe2(C5H5)2(CN)2(CNMe2}2] zwitterions (L = CO or organoisocyanide) and their reactions with alkyl and protic electrophiles, *J. Organomet. Chem*. **1996**, *509*, 197-207. (f) Albano, V. G.; Busetto, L.; Marchetti, F.; Monari, M.; Zanotti, V. Acetonitrile activation in di-iron μ-carbyne complexes: synthesis and structure of the cyanomethyl complex [Fe2(CNMe2)(μ-CO)(CO)(CH2CN)(Cp)2]. *J. Organomet. Chem*. **2002**, *649*, 64-69. (g) Marchetti, F.; Zacchini, S.; Zanotti, V. C-N Coupling of Isocyanide Ligands Promoted by Acetylide Addition to Diiron Aminocarbyne Complexes. *Organometallics* **2015**, *34*, 3658−3664.

35 (a) Albano, V. G.; , Busetto, L.; Camiletti, C.; Castellari, C.; Monari, M.; Zanotti, V., Selective C-C bond formation at diiron aminocarbyne complexes, *J. Chem. Soc., Dalton Trans.*, **1997**, 4671–4676. (b) Busetto, L.; Marchetti, F.; Mazzoni, R.; Salmi, M.; Zacchini, S.; Zanotti, V. SPh functionalized bridging-vinyliminium diiron and diruthenium complexes, *J. Organomet. Chem*. **2008**, *693*, 3191–3196.

36 Natori, I.; Natori, S.; Sekikawa, H.; Ogino, K. Synthesis of C60 end-capped poly(4-diphenylaminostyrene): Addition of poly(4-diphenylaminostyryl)lithium to C60, *Reactive & Functional Polymers* **2009**, *69*, 613–618.

37 Skoog, D. A.; West, D. M.; Holler, F. J. Fundamentals of Analytical Chemistry, 7th Edition, Thomson Learning, Inc, USA, 1996.

38 Willker, W.; Leibfritz, D.; Kerssebaum, R.; Bermel, W., Gradient selection in inverse heteronuclear correlation spectroscopy, *Magn. Reson. Chem*. **1993**, *31*, 287-292.

39 Neese, F. The ORCA program system. Wiley Interdiscip. Rev. Comput. Mol. Sci. **2012**, *2*, 73−78; Neese, F. Software update: The ORCA program system, version 4.0. Wiley Interdiscip. Rev. Comput. Mol. Sci. **2018**, *8*:e1327.

40 Becke, A. D. Density-functional thermochemistry. V. Systematic optimization of exchange-correlation functionals. *J. Chem. Phys.* **1997**, *107*, 8554–8560.

41 Grimme, S.; Antony, J.; Ehrlich, S.; Krieg, H. A consistent and accurate ab initio parametrization of density functional dispersion correction (DFT-D) for the 94 elements H-Pu. *J. Chem. Phys*. **2010**, *132*, 154104.

42 Sheldrick, G. M. SADABS-2008/1 - Bruker AXS Area Detector Scaling and Absorption Correction, Bruker AXS: Madison, Wisconsin, USA, **2008**

43 Sheldrick, G. M. *Acta Crystallogr. C*, **2015**, *71*, 3.